

# Leptonic $\mu$ - and $\tau$ -decays: mass effects, polarization effects and $O(\alpha)$ radiative corrections

M. Fischer, S. Groote, J.G. Körner and M.C. Mauser

Institut für Physik, Johannes Gutenberg-Universität  
Staudinger Weg 7, D-55099 Mainz, Germany

## Abstract

We calculate the radiative corrections to the unpolarized and the four polarized spectrum and rate functions in the leptonic decay of a polarized  $\mu$  into a polarized electron. The new feature of our calculation is that we keep the mass of the final state electron finite which is mandatory if one wants to investigate the threshold region of the decay. Analytical results are given for the energy spectrum and the polar angle distribution of the final state electron whose longitudinal and transverse polarization is calculated. We also provide analytical results on the integrated spectrum functions. We analyze the  $m_e \rightarrow 0$  limit of our general results and investigate the quality of the  $m_e \rightarrow 0$  approximation. In the  $m_e \rightarrow 0$  case we discuss in some detail the role of the  $O(\alpha)$  anomalous helicity flip contribution of the final electron which survives the  $m_e \rightarrow 0$  limit. The results presented in this paper also apply to the leptonic decays of polarized  $\tau$ -leptons for which we provide numerical results.

# 1 Introduction

While calculating the radiative  $O(\alpha_s)$  QCD corrections to polarization effects in semileptonic decays of heavy quarks, where the full quark mass dependence was retained [1, 2], we came to realize that our results could also be gainfully employed in the corresponding  $O(\alpha)$  QED corrections to the weak leptonic decays of the  $\mu^-$  and  $\tau^-$ -leptons<sup>1</sup>. In most of the previous radiative correction calculations the mass of the charged lepton daughter  $l'$  has been neglected except for anomalous contributions from the collinear region which survive the  $m_{l'} \rightarrow 0$  limit [3, 4, 5] and the logarithmic terms  $\sim (\ln m_{l'})$  which are needed to regularize the collinear divergencies that appear in the loop and tree graph (“internal bremsstrahlung”) contributions. These logarithmic terms partially cancel in the spectrum and completely cancel in the rate when the loop and tree graph contributions are added.

From general considerations it follows that the unpolarized and three of the polarized spectrum functions contain only even powers of the mass ratio  $m_{l'}/m_l$ . Considering the fact that  $(m_e/m_\mu)^2 = 2.34 \cdot 10^{-5}$ ,  $(m_\mu/m_\tau)^2 = 3.54 \cdot 10^{-3}$  and  $(m_e/m_\tau)^2 = 8.27 \cdot 10^{-8}$  the zero mass approximation should be a good approximation for most of the energy spectrum of the daughter leptons except for the region close (or very close) to the soft endpoint of the spectrum (also referred to as the threshold region) where finite mass effects have to be retained. Contrary to this the transverse polarization of the daughter lepton is proportional to the linear mass ratio  $m_{l'}/m_l$ . Also, when integrating the spectrum functions, the linear mass ratio enters in all four polarized rate functions. Finite mass corrections may thus play an important role at least for  $(\tau \rightarrow \mu)$ -decays where the linear mass ratio  $m_\mu/m_\tau = 5.95 \cdot 10^{-2}$  is not very small. An improved analysis of  $\tau$ -decays is of quite some topical interest since large samples of  $\tau$ -leptons are currently being produced at the existing two  $B$  factories in Japan and in the USA, and are expected to be produced at future  $\tau$ -charm factories to be set up in Ithaca and Beijing. As the data becomes more precise, the predictions of the SM including also radiative correction effects will be tested at an ever-rising level of precision. It is then evident that the inclusion of final lepton mass effects must play an important role in particular in the threshold region.

We determine the radiative corrections to the daughter’s lepton energy spectrum and its longitudinal and transverse polarization keeping the dependence on the polarization of the parent lepton. This generalizes the calculation of [6] in which the zero mass approximation was used. Our calculation extends the calculation of [7], which also includes finite mass effects, in that we include the longitudinal and transverse polarization of the daughter lepton.

---

<sup>1</sup>The three leptonic  $\mu^-$  and  $\tau^-$ -decays are treated within the Standard Model, i.e. they are all governed by the same  $(V - A)$  coupling structure and coupling strength  $G_F$ .

The paper is structured as follows. In Sec. 2 we introduce our notation and write down the general structure of the spin-dependent rate. Sec. 3 contains our Born term results.  $W$ -propagator effects are taken into account in Sec. 4. In Sec. 5 we present our analytical and numerical results on the  $O(\alpha)$  radiative corrections. In Sec. 6 we consider the  $m_l' \rightarrow 0$  limit of the  $m_l' \neq 0$  results presented in Sec. 5 and discuss in some detail the origin of the anomalous helicity flip contribution. Sec. 7 contains our summary and conclusions. In two Appendices we collect some technical material on trigonometric functions and Fierz identities relevant to our calculation.

## 2 General structure of spin-dependent rate

To make life simple we shall in the following always refer to the specific case  $\mu^- \rightarrow e^- + \bar{\nu}_e + \nu_\mu$  instead of referring to the generic case involving also leptonic  $\tau$ -decays when writing down analytical results. Of course, when discussing numerical results, the two leptonic  $\tau$ -decay channels  $\tau^- \rightarrow \mu^- + \bar{\nu}_\mu + \nu_\tau$  and  $\tau^- \rightarrow e^- + \bar{\nu}_e + \nu_\tau$  are also included.

Since the subject of  $\mu^-$ -decays is extensively covered in the relevant textbooks (see e.g. Refs. [8, 9, 10]) and review articles (see e.g. Refs. [11, 12, 13]) we can afford to be very brief in describing the formalism.

From helicity counting one knows that there are altogether five spin-dependent structure functions and one spin-independent structure function describing the leptonic decay of a polarized muon into a polarized electron. We thus define a spin-dependent differential rate in terms of six invariant structure functions  $A_i$ . In the rest system of the  $\mu^-$  the decay distribution reads

$$\begin{aligned} \frac{d\Gamma}{dx d\cos\theta_P} = \beta x \Gamma_0 \left( A_1 + \frac{1}{m_\mu} A_2 (p_e \cdot s_\mu) + \frac{1}{m_\mu} A_3 (p_\mu \cdot s_e) + \frac{1}{m_\mu^2} A_4 (p_e \cdot s_\mu) (p_\mu \cdot s_e) \right. \\ \left. + A_5 (s_\mu \cdot s_e) + \frac{1}{m_\mu^2} A_6 \epsilon_{\alpha\beta\gamma\delta} p_\mu^\alpha p_e^\beta s_\mu^\gamma s_e^\delta \right). \end{aligned} \quad (1)$$

As usual  $x = 2E_e/m_\mu$  denotes the scaled energy of the electron where the energy of the electron is defined in the rest frame of the  $\mu^-$ .  $\theta_P$  is the polar angle between the polarization of the muon and the momentum direction of the electron in the muon rest frame.

Eq. (1) will be evaluated in the rest system of the muon where  $p_\mu = (m_\mu; 0, 0, 0)$  and  $p_e = (E_e; 0, 0, |\vec{p}_e|) = (m_\mu/2)(x; 0, 0, x\beta)$ . The velocity of the electron is denoted

by  $\beta = \sqrt{1 - 4y^2/x^2}$  where  $y = m_e/m_\mu$ . In the rest frame of the  $\mu^-$  the polarization four-vectors of the  $\mu^-$  and  $e^-$  are given by

$$s_\mu^\alpha = (0; \vec{\zeta}_\mu), \quad (2)$$

$$s_e^\alpha = \left( \frac{\vec{n}_e \cdot \vec{p}_e}{m_e}; \vec{n}_e + \frac{\vec{n}_e \cdot \vec{p}_e}{m_e(E_e + m_e)} \vec{p}_e \right), \quad (3)$$

where the polarization three-vector  $\vec{\zeta}_\mu$  of the  $\mu^-$  and the quantization axis  $\vec{n}_e$  of the spin of the  $e^-$  in their respective rest frames read (see Fig. 1)

$$\vec{\zeta}_\mu = (\sin \theta_P, 0, \cos \theta_P) \quad (4)$$

and

$$\vec{n}_e = (\sin \theta \cos \chi, \sin \theta \sin \chi, \cos \theta). \quad (5)$$

Eq. (4) holds for 100% polarized muons. For partially polarized muons with magnitude of polarization  $P$  the representation (4) has to be multiplied by  $P$  such that  $\vec{P}_\mu = P\vec{\zeta}_\mu$ . The representation Eq. (5) needs a word of explanation. The vector  $\vec{n}_e$  denotes the orientation of the quantization axis of the electron's spin in the rest frame of the electron which can be freely chosen. The orientation of  $\vec{n}_e$  has no physical meaning per se. In particular  $\vec{n}_e$  is *not* the polarization vector  $\vec{P}_e$  of the electron whose Cartesian components can, however, be obtained by projecting onto the  $x$ -axis ( $\theta = \pi/2, \chi = 0$ ), the  $y$ -axis ( $\theta = \pi/2, \chi = \pi/2$ ) and the  $z$ -axis ( $\theta = 0$ ).

One finally has [6, 14]

$$\begin{aligned} \frac{d\Gamma}{dx d\cos \theta_P} &= \beta x \Gamma_0 (G_1 + G_2 P \cos \theta_P + G_3 \cos \theta + G_4 P \cos \theta_P \cos \theta \\ &+ G_5 P \sin \theta_P \sin \theta \cos \chi + G_6 P \sin \theta_P \sin \theta \sin \chi). \end{aligned} \quad (6)$$

The relation between the invariant structure functions  $A_i$  and the frame-dependent spectrum functions  $G_i$  is given by

$$\begin{aligned} G_1 &= A_1, \\ G_2 &= -\frac{1}{2}x\beta A_2, \end{aligned}$$

$$\begin{aligned}
G_3 &= \frac{1}{2y}x\beta A_3, \\
G_4 &= -\frac{1}{4y}x^2\beta^2 A_4 - \frac{1}{2y}xA_5, \\
G_5 &= -A_5, \\
G_6 &= \frac{1}{2}x\beta A_6.
\end{aligned} \tag{7}$$

$G_1$  is the unpolarized spectrum function,  $G_2$  and  $G_3$  are single spin polarized spectrum functions referring to the spins of the  $\mu^-$  and  $e^-$ , resp., and  $G_4$ ,  $G_5$  and  $G_6$  describe spin-spin correlations between the spin vectors of the muon and electron<sup>2</sup>.  $G_6$  represents a so-called  $T$ -odd observable. This is evident when rewriting the angular factor multiplying  $G_6$  in (6) in triple-product form, i.e.  $\sin\theta_P \sin\theta \sin\chi = |\vec{p}_e|^{-1} \vec{p}_e \cdot (\vec{\zeta}_\mu \times \vec{n}_e)$ .  $G_6$  is identically zero in the SM since, on the one hand, the weak coupling constant  $G_F$  is real and, on the other hand, the loop contributions do not generate imaginary parts.  $G_6$  will therefore not be discussed any further in the following.

It is quite instructive to rewrite Eq. (6) in a factorized form

$$\frac{d\Gamma}{dx d\cos\theta_P} = \beta x \Gamma_0 (G_1 + G_2 P \cos\theta_P) (1 + \vec{P}_e \cdot \vec{n}_e) \tag{8}$$

A comparison with Eq. (6) shows that the polarization vector  $\vec{P}_e$  of the electron has the components

$$\begin{aligned}
P_e^x &:= P_e^\perp = \frac{P G_5 \sin\theta_P}{G_1 + G_2 P \cos\theta_P}, \\
P_e^y &:= P_e^N = \frac{P G_6 \sin\theta_P}{G_1 + G_2 P \cos\theta_P}, \\
P_e^z &:= P_e^l = \frac{G_3 + G_4 P \cos\theta_P}{G_1 + G_2 P \cos\theta_P}.
\end{aligned} \tag{9}$$

We have as usual denoted the  $(x, y, z)$  components of  $\vec{P}_e$  by  $(P_e^\perp, P_e^N, P_e^l)$  where  $(\perp, N, l)$  stand for the polarization components transverse to the momentum direction of the electron (in the plane spanned by the momentum of the electron and the polarization vector

---

<sup>2</sup>The spectrum function  $G_5$  describing the transverse polarization of the electron vanishes for vanishing electron mass and is therefore not included in the corresponding decay distribution in [6].

of the muon), normal to this plane and longitudinal, respectively. Eq. (9) shows that the spectrum functions  $G_3$  and  $G_4$  determine the longitudinal polarization of the electron while its transverse polarization (in the plane spanned by the electron's momentum and the muon's polarization) is determined by  $G_5$ <sup>3</sup>.

The limits on  $x = 2E_e/m_\mu$  are given by  $x_{min} = 2y$  and  $x_{max} = 1 + y^2$  where, as before,  $y = m_e/m_\mu$ .  $\Gamma_0$ , finally, is the  $m_e = 0$  Born term rate given by  $\Gamma_0 = G_F^2 m_\mu^5 / 192\pi^3$ . The differential rate for the charge conjugated decay  $\mu^+ \rightarrow e^+ + \nu_e + \bar{\nu}_\mu$  is obtained from Eq. (6) by the substitution  $G_i \rightarrow G_i$  ( $i = 1, 4, 5, 6$ ) and  $G_i \rightarrow -G_i$  ( $i = 2, 3$ ).

It is convenient to split the unpolarized and polarized rate functions into a Born term part and a radiatively corrected part according to

$$G_i = G_i^{Born} + G_i^{(\alpha)} \quad i = 1, 2, 3, 4, 5. \quad (10)$$

The respective results on the Born term contributions  $G_i^{Born}$  and the  $O(\alpha)$  corrections to the rate functions  $G_i^{(\alpha)}$  are given in Secs. 3 and 5. The sum of the two contributions in Eq. (10) will generally be referred to as the next-to-leading order (NLO) result.

### 3 Born term results

We shall work with the charge retention form of the Lagrangian for the decay  $\mu^- \rightarrow e^- + \bar{\nu}_e + \nu_\mu$  which reads<sup>4, 5</sup>

$$\mathcal{L}(x) = \frac{G_F}{\sqrt{2}} \bar{\Psi}_e(x) \gamma^\alpha (\mathbb{1} - \gamma_5) \Psi_\mu(x) \bar{\Psi}_{\nu_\mu}(x) \gamma_\alpha (\mathbb{1} - \gamma_5) \Psi_{\nu_e}(x) + h.c. \quad (11)$$

When squaring the corresponding matrix element one obtains the tensor  $C^{\alpha\beta}$  from the charged lepton side ( $C$  for charged) which has to be contracted with the neutrino-side tensor  $N^{\alpha\beta}$  ( $N$  for neutral). For the Born term contribution of the charge-side tensor one obtains

---

<sup>3</sup>As noted before in the SM there is no transverse polarization normal to that plane.

<sup>4</sup>The charge retention form of the Lagrangian is obtained from the usual Standard Model charged current-current form through the Fierz transformation (B1) written down in Appendix B. The minus sign from the Fierz identity is cancelled from having to commute the Fermion fields an odd number of times in order to relate the two forms. Note that the Fierz identity is a four-dimensional identity. Since our calculations are done in four dimensions the Fierz identity can be safely applied.

<sup>5</sup>When the Lagrangian for  $\mu$ -decay is written in charge retention form the similarity of the decay  $\mu^- \rightarrow e^- + \bar{\nu}_e + \nu_\mu$  to the decay  $b \rightarrow c + e^- + \bar{\nu}_e$  becomes quite apparent through the substitutions  $b \leftrightarrow \mu^-$ ,  $c \leftrightarrow e^-$ ,  $e^- \leftrightarrow \nu_\mu$  and  $\bar{\nu}_e \leftrightarrow \bar{\nu}_e$ .

$$C_{Born}^{\alpha\beta} = \frac{1}{4} \text{Tr} \left\{ (\not{p}_e + m_e) (\mathbb{1} + \gamma_5 \not{p}_e) \gamma^\alpha (\mathbb{1} - \gamma_5) (\not{p}_\mu + m_\mu) (\mathbb{1} + \gamma_5 \not{p}_\mu) \gamma^\beta (\mathbb{1} - \gamma_5) \right\}, \quad (12)$$

where the dependence on the polarization four-vectors of the  $\mu^-$  and  $e^-$  has been retained.

Since only even-numbered  $\gamma$ -matrix strings survive between the two  $(\mathbb{1} - \gamma_5)$ -factors in Eq. (12) one can compactly write the result of the trace evaluation as

$$C_{Born}^{\alpha\beta} = 2(\bar{p}_\mu^\beta \bar{p}_e^\alpha + \bar{p}_\mu^\alpha \bar{p}_e^\beta - g^{\alpha\beta} \bar{p}_\mu \cdot \bar{p}_e + i\epsilon^{\alpha\beta\gamma\delta} \bar{p}_{e,\gamma} \bar{p}_{\mu,\delta}), \quad (13)$$

where

$$\bar{p}_\mu^\alpha = p_\mu^\alpha - m_\mu s_\mu^\alpha, \quad (14)$$

$$\bar{p}_e^\alpha = p_e^\alpha - m_e s_e^\alpha \quad (15)$$

and where  $s_\mu^\alpha$  and  $s_e^\alpha$  are the polarization four-vectors of the  $\mu^-$  and  $e^-$ , resp., defined in Eq. (2).

The dependence on the momentum directions of the  $\bar{\nu}_e$ - and  $\nu_\mu$ -neutrinos has been completely integrated out in the differential rate. Thus the neutrino-side of the interaction can only depend on the spatial piece of the second rank tensor build from the momentum transfer to the neutrinos (for the present purpose the neutrinos are treated as massless) which we denote by  $Q^\alpha$ <sup>6</sup>. Thus the relevant neutral-side tensor is given by

$$N^{\alpha\beta} = -g^{\alpha\beta} + \frac{Q^\alpha Q^\beta}{Q^2}. \quad (16)$$

The Born spectrum functions can then be extracted from

$$Q^2 N^{\alpha\beta} C_{\alpha\beta}^{Born} = 2((\bar{p}_\mu \cdot \bar{p}_e) Q^2 + 2(\bar{p}_\mu \cdot Q)(\bar{p}_e \cdot Q)), \quad (17)$$

where the antisymmetric piece in  $C_{\alpha\beta}^{Born}$  has dropped out after the symmetric contraction. At the Born term level one has  $Q = p_\mu - p_e$ .

Including the correct normalization the differential Born term rate is given by

$$\frac{d\Gamma^{Born}}{dx d\cos\theta_P} = \Gamma_0 \beta x \frac{Q^2 N^{\alpha\beta} C_{\alpha\beta}^{Born}}{m_\mu^4}. \quad (18)$$

---

<sup>6</sup>We denote the momentum transfer to the neutrino pair by a capital  $Q$  in order to set it apart from the momentum transfer  $q$  to the  $(e^- \bar{\nu}_e)$ -pair used in Sec. 4.

The spectrum functions defined in Eq. (6) can then easily be calculated from the Born term contributions (17) using the relations Eq. (7). They are given by

$$\begin{aligned}
G_1^{Born} &= x(3 - 2x) - (4 - 3x)y^2, \\
G_2^{Born} &= \beta x(1 - 2x + 3y^2), \\
G_3^{Born} &= -\beta x(3 - 2x + y^2), \\
G_4^{Born} &= -x(1 - 2x) - (4 + x)y^2, \\
G_5^{Born} &= -2y(1 - x + y^2).
\end{aligned} \tag{19}$$

Note that the Born term spectrum functions  $G_{1,2,3,4}^{Born}$  and  $G_5^{Born}/y$  are quadratically dependent on  $y$ . This is in agreement with the general arguments presented in [15]. For  $y^2 = 0$  ( $m_e = 0$ ) one has  $G_1^{Born} = -G_3^{Born}$  and  $G_2^{Born} = -G_4^{Born}$  which reflects the fact that a mass zero left-chiral electron is purely lefthanded. The Born term results (19) reproduce the  $y = 0$  results of Ref. [6]. For  $y^2 \neq 0$  ( $m_e \neq 0$ ) our Born term results for  $G_1^{Born}$  and  $G_2^{Born}$  agree with those of Ref. [7]. Note that the spectrum function  $G_5^{Born}$  is proportional to  $y$  and thus vanishes for vanishing electron mass. The overall chiral factor  $y = m_e/m_\mu$  in  $G_5$  originates from a lefthanded/righthanded interference contribution which is chirally suppressed.

In Figs. 2a ( $\mu \rightarrow e$ ), 3a ( $\tau \rightarrow \mu$ ) and 4a ( $\tau \rightarrow e$ ) we show plots of the  $x$ -dependence of the four Born term spectrum functions  $\beta x G_{1,2,3,4}^{Born}$ . They rise and fall from zero at the soft end of the spectrum to  $(1 - y^2)^3$  ( $i = 1, 4$ ) and  $-(1 - y^2)^3$  ( $i = 2, 3$ ) at the hard end of the spectrum, respectively. The  $m_\nu = 0$  pattern  $G_1^{Born} = -G_3^{Born}$  and  $G_2^{Born} = -G_4^{Born}$  is slightly distorted by final lepton mass effects except for the point  $x_{max} = 1 + y^2$  where the above  $m_\nu = 0$  relations are exact. For the spectrum function  $G_5^{Born}$  one finds  $G_5^{Born}(x_{min} = 2y) = -2y(1 - y)^2$  and  $G_5^{Born}(x_{max} = 1 + y^2) = 0$ . The chirally suppressed contribution of  $\beta x G_5^{Born}$  is negative over the whole  $x$ -range. At the scale of the plots it is only visible for the case  $\tau \rightarrow \mu$  (Fig. 3a).

In addition to the polarization observables we also define a forward-backward asymmetry for the case that the spin of the electron is not observed. It reads

$$A_{FB} = \frac{\Gamma_F - \Gamma_B}{\Gamma_F + \Gamma_B} = \frac{1}{2} P \frac{G_2}{G_1}, \tag{20}$$

where  $\Gamma_F$  and  $\Gamma_B$  are the rates into the forward ( $\cos \theta_P \geq 0$ ) and backward ( $\cos \theta_P \leq 0$ ) hemispheres.

One can also define a forward–backward asymmetry of the longitudinal polarization proportional to  $G_4/G_1$  according to

$$P_{\nu}^{l(FB)} = \frac{\Gamma_F^+ - \Gamma_F^- - \Gamma_B^+ + \Gamma_B^-}{\Gamma_F^+ + \Gamma_F^- + \Gamma_B^+ + \Gamma_B^-} = \frac{1}{2} P \frac{G_4}{G_1}, \quad (21)$$

where the indices  $+/-$  denote the helicities of the electron. This asymmetry will be difficult to measure since it involves a spin–spin correlation measurement. We shall therefore not discuss this asymmetry any further in this paper.

The longitudinal polarization and the forward–backward asymmetry take the values  $P_e^{l,Born} = -\frac{1}{3}P \cos \theta_P$  and  $A_{FB}^{Born} = 0$ , respectively, at the lower limit  $x_{min} = 2y$  where  $G_1^{Born} = -3G_4^{Born}$  and  $G_2^{Born} = G_3^{Born} = 0$ . This has to be contrasted with the naive limits  $P_e^{l,Born} = -1$  and  $A_{FB}^{Born} = \frac{1}{6}P$  when naively setting  $y = 0$  in the corresponding ratios. At the upper limit  $x_{max} = (1 + y^2)$ , where  $G_1^{Born} = -G_2^{Born} = -G_3^{Born} = G_4^{Born} = (1 - y^2)^2$ , the longitudinal polarization decreases to  $P_e^{l,Born} = -1$  irrespective of the value of  $P \cos \theta_P$ , and the forward–backward asymmetry decreases to  $A_{FB}^{Born} = -\frac{1}{2}P$  as in the naive  $m_e = 0$  case. At the soft end of the spectrum one finds a substantial transverse polarization  $P_e^{\perp,Born} = -\frac{1}{3}P \sin \theta_P$  which is independent of  $y$  contrary to naive expectations. Thus the total polarization of the electron at threshold is given by  $|\vec{P}_e^{Born}| = \frac{1}{3}P$  irrespective of the value of  $\cos \theta_P$ . At the hard end of the spectrum one has  $P_e^{\perp,Born} = 0$ .

In Figs. 2b ( $\mu \rightarrow e$ ), 3b ( $\tau \rightarrow \mu$ ) and 4b ( $\tau \rightarrow e$ ) we show the  $x$ –dependence of the Born term prediction for the longitudinal and transverse polarization of the daughter lepton. We set  $P = 1$  and take three values  $\cos \theta_P = 1, 0$  and  $-1$  for the longitudinal polarization and set  $\cos \theta_P = 0$  for the transverse polarization. The longitudinal polarization stays close to  $-1$  over most of the (hard part) of the spectrum but deviates significantly from the naive value  $-1$  in the threshold region with only a slight dependence on the value of  $\cos \theta_P$ . In order to highlight the deviations from the naive value  $P_{\nu}^{l,Born} = -1$  in the threshold region we have chosen logarithmic scales for the energy variable  $x$ . The transverse polarization is negative and stays very close to zero over most of the (hard part) of the spectrum and decreases to its limiting value  $-1/3$  at threshold. In fact all the Born term curves can be seen to approach the limits discussed above at the soft and hard end of the spectrum.

In Figs. 2c, 3c and 4c we show the corresponding curves for the forward–backward asymmetry  $A_{FB}^{Born}$  for the three decay cases. Again we set  $P = 1$ . The forward–backward asymmetries rise from the limiting value  $A_{FB}^{Born} = 0$  at threshold and then fall to  $A_{FB}^{Born} = -1/2$  at the hard end of the spectrum.

Next we integrate the differential Born term rates over the full  $x$  spectrum. Let us define reduced Born rate functions  $\hat{G}_i^{Born}$  according to

	$\mu \rightarrow e$		$\tau \rightarrow \mu$		$\tau \rightarrow e$	
	Born	$(\alpha)$	Born	$(\alpha)$	Born	$(\alpha)$
$\hat{G}_1$	-0.019%	-0.12%	-2.82%	- 8.48%	$-6.62 \cdot 10^{-5}\%$	$-7.39 \cdot 10^{-4}\%$
$\hat{G}_2$	$-3.57 \cdot 10^{-4}\%$	-0.67%	-0.57%	-11.23%	$-7.60 \cdot 10^{-8}\%$	-0.039%
$\hat{G}_3$	-0.031%	-1.48%	-4.25%	-24.49%	$-1.10 \cdot 10^{-4}\%$	-0.084%
$\hat{G}_4$	-0.019%	-1.43%	-2.82%	-22.15%	$-6.62 \cdot 10^{-5}\%$	-0.083%

**Table 1:**

Percentage mass corrections to  $m_{\nu} = 0$  (Born) and  $m_{\nu} \rightarrow 0$  ( $O(\alpha)$ ) rate functions for the three cases ( $\mu \rightarrow e$ ), ( $\tau \rightarrow \mu$ ) and ( $\tau \rightarrow e$ ).

$$\hat{G}_i^{Born} = \int_{2y}^{1+y^2} dx \beta x G_i^{Born} \quad i = 1, 2, 3, 4. \quad (22)$$

One obtains

$$\begin{aligned} \hat{G}_1^{Born} &= \frac{1}{2}(1 - y^4)(1 - 8y^2 + y^4) - 12y^4 \ln y = \frac{1}{2} - 4y^2 + O(y^4), \\ \hat{G}_2^{Born} &= -\frac{1}{6}(1 - y)^5(1 + 5y + 15y^2 + 3y^3) = -\frac{1}{6} + \frac{16}{3}y^3 + O(y^4), \\ \hat{G}_3^{Born} &= -\frac{1}{6}(1 - y)^5(3 + 15y + 5y^2 + y^3) = -\frac{1}{2} + \frac{20}{3}y^2 - 16y^3 + O(y^4), \\ \hat{G}_4^{Born} &= \frac{1}{6}(1 - y^4)(1 - 8y^2 + y^4) - 4y^4 \ln y = \frac{1}{6} - \frac{4}{3}y^2 + O(y^4), \\ \hat{G}_5^{Born} &= -y\left(\frac{1}{3}(1 - y^2)(1 + 10y^2 + y^4) + 4y^2(1 + y^2) \ln y\right) = -y\left(\frac{1}{3} + (3 + 4 \ln y)y^2 + O(y^4)\right) \end{aligned} \quad (23)$$

The occurrence of odd powers of  $y$  in  $\hat{G}_2^{Born}$  and  $\hat{G}_3^{Born}$  can be traced to the lower boundary  $x = 2y$  of the  $x$ -integration which is linear in  $y$ . In view of this it is quite remarkable that  $\hat{G}_1^{Born}$ ,  $\hat{G}_4^{Born}$  and  $\hat{G}_5^{Born}/y$  contain only even powers of  $y$ . Nevertheless, the leading mass correction to  $\hat{G}_3^{Born}$  sets in only at  $O(y^2)$  and, for  $\hat{G}_2^{Born}$ , only at  $O(y^3)$ . In this sense the Born term rates are well protected against finite electron mass effects, or, in the case ( $\tau \rightarrow \mu$ ), reasonably well against muon mass effects. This is illustrated in Table 1 where we list the values of the Born term percentage changes  $(\hat{G}_i(m \neq 0) - \hat{G}_i(m = 0)) / \hat{G}_i(m = 0)$  when going from  $m_{\nu} = 0$  to  $m_{\nu} \neq 0$  for all three cases.

The average longitudinal polarization of the electron  $\langle P_e^l \rangle$  and the average forward–backward asymmetry  $\langle A_{FB} \rangle$  is obtained by the replacement ( $G_i \rightarrow \hat{G}_i$ ) in (9) and (20). As in the rate expressions (23) the final state lepton mass effects on the Born term polarization  $\langle P_e^l \rangle$  and forward–backward asymmetry  $\langle A_{FB} \rangle$  are quite small. The deviation from the  $m_{l'} = 0$  result  $\langle P_{l'}^l \rangle = -1$  is of  $O(10^{-4})$  in muon decay and  $O(10^{-6})$  in ( $\tau \rightarrow e$ ). For ( $\tau \rightarrow \mu$ ) the deviation from  $\langle P_\mu^l \rangle = -1$  is of  $O(10^{-2})$ . The dependence on the value of  $P \cos \theta_P$  is very small. The average value of the forward–backward asymmetry  $\langle A_{FB} \rangle$  is quite close ( $O(10^{-2} - 10^{-3})$ ) to the  $y = 0$  prediction  $\langle A_{FB} \rangle = -1/6$ . The average transverse polarization  $\langle P_\mu^\perp \rangle$  is generally quite small due to the overall chiral factor  $y = m_{l'}/m_l$ . To be specific, for  $\theta_P = \pi/2$  one finds an average transverse polarization of  $-0.3\%$ ,  $-3.7\%$  and  $-0.02\%$  for the three cases ( $\mu \rightarrow e$ ), ( $\tau \rightarrow \mu$ ) and ( $\tau \rightarrow e$ ), respectively.

## 4 $W$ -boson propagator effects

In order to incorporate  $W$ -boson propagator effects one has to rewrite the charge retention form of the four–Fermi interaction (11) in terms of the charged currents of the Standard Model including the  $W$ -boson propagator. This is easily done using the Fierz transformation property written down in Eq. (B1) in Appendix B.

For the present purposes it is only necessary to take into account  $W$ -boson propagator effects in the Born term contributions. The momentum transfer is now  $q = p_\mu - p_{\nu_\mu} = p_e + p_{\nu_e}$ . The  $q^\mu q^\nu$  piece of the  $W$ -boson propagator contributes only at  $O(m_e^2 m_\mu^2 / m_W^4)$  in the spectrum and rate functions and can therefore be dropped. In fact, using the Fierz identity (B2), it is not difficult to compute the contribution of the  $q^\mu q^\nu$  piece exactly. The  $W$ -boson propagator effect on the spectrum can thus be taken into account by the replacement

$$1 \rightarrow \left( \frac{m_W^2}{q^2 - m_W^2} \right)^2 \approx 1 + \frac{m_\mu^2}{m_W^2} \frac{x(2-x)}{3-2x} \quad i = 1, 3 \quad , \quad (24)$$

$$\approx 1 - \frac{m_\mu^2}{m_W^2} \frac{x^2}{1-2x} \quad i = 2, 4 \quad . \quad (25)$$

where terms of  $O(m_e^2/m_W^2)$  have been neglected. Numerically the propagator corrections are quite small since  $m_\mu^2/m_W^2 = 1.73 \cdot 10^{-6}$  and  $m_\tau^2/m_W^2 = 4.88 \cdot 10^{-4}$ .

As is evident from Eq. (24) the  $W$ -boson propagator affects the two pairs of spectrum functions differently. This means that one cannot absorb the  $W$ -boson propagator effect entirely into a redefinition of Fermi's coupling constant  $G_F$ , as advocated in Refs. [16, 17], when one considers polarization effects.

In order to determine the propagator corrections to the rate functions one has to do the integrations

$$\int_0^1 dx x G_{1,3}^{Born} \left( 1 + \frac{m_\mu^2}{m_W^2} \frac{x(2-x)}{3-2x} \right) = \pm \frac{1}{2} \left( 1 + \frac{3}{5} \frac{m_\mu^2}{m_W^2} \right), \quad (26)$$

$$\int_0^1 dx x G_{2,4}^{Born} \left( 1 - \frac{m_\mu^2}{m_W^2} \frac{x^2}{1-2x} \right) = \mp \frac{1}{6} \left( 1 + \frac{1}{5} \frac{m_\mu^2}{m_W^2} \right), \quad (27)$$

where terms of  $O(y)$  have been dropped in the Born term factors and in the integration measure. Again it is evident from Eq. (26) and Eq. (27) that the  $W$ -boson propagator affects the two pairs of rate functions differently. If the  $W$ -boson propagator effect is absorbed into a redefinition of  $G_F$  using a measurement of the total unpolarized rate then this must be compensated for by multiplying the polarization dependent pieces  $\hat{G}_{2,4}$  by  $(1 - \frac{2}{5} \frac{m_\mu^2}{m_W^2})$  when calculating the average of the longitudinal polarization of the electron  $\langle P_e^l \rangle$  or the forward-backward asymmetry  $\langle A_{FB} \rangle$ .

## 5 $O(\alpha)$ corrections to spin dependent rate functions

Many of the technical ingredients that go into the calculation of the  $O(\alpha)$  corrections can be found in a detailed account of the  $O(\alpha_s)$  corrections to the decay of a polarized top into a bottom quark and a  $W$  gauge boson  $t \rightarrow b + W^+$  presented in Ref. [2] (for the loop contribution see also [18]). Compared to Ref. [2] one needs to include the polarization dependence of the final massive fermion in this application. For the  $O(\alpha)$  tree-graph and one-loop contributions this is easily done.

Let us briefly discuss the tree graph contribution. The  $O(e)$  tree graph amplitude (“internal bremsstrahlung”) consists of the two contributions where the photon is either radiated off the electron or off the muon. One thus has

$$\mathcal{M}^\alpha = e \bar{u}_e \left( \gamma_\delta \frac{\not{p}_e + \not{k} + m_e}{(p_e + k)^2 - m_e^2} \gamma^\alpha (\mathbb{1} - \gamma_5) + \gamma^\alpha (\mathbb{1} - \gamma_5) \frac{\not{p}_\mu - \not{k} + m_\mu}{(p_\mu - k)^2 - m_\mu^2} \gamma_\delta \right) u_\mu \epsilon^{*\delta}, \quad (28)$$

where  $k$  and  $\epsilon_\delta$  are the momentum and the polarization four-vector of the photon. Four-momentum conservation now reads  $p_\mu = p_e + Q + k$  where  $Q$  is again the momentum transferred to the neutrino pair. When squaring the tree graph amplitude one only sums over the polarization states of the photon since the muon and the electron are taken as polarized. Omitting again the antisymmetric contribution one obtains in the Feynman gauge

$$\begin{aligned}
C^{(\alpha)\alpha\beta} &= \sum_{\gamma\text{-spin}} \mathcal{M}^\alpha \mathcal{M}^{\beta\dagger} = \frac{e^2}{2} \left\{ \frac{1}{(k \cdot p_e)} \left( \frac{k \cdot \bar{p}_e - m_e^2}{(k \cdot p_e)} + \frac{p_\mu \cdot \bar{p}_e}{(k \cdot p_\mu)} \right) (k^\alpha \bar{p}_\mu^\beta + k^\beta \bar{p}_\mu^\alpha - k \cdot \bar{p}_\mu g^{\alpha\beta}) \right. \\
&+ \frac{1}{(k \cdot p_\mu)} \left( \frac{k \cdot \bar{p}_\mu + m_\mu^2}{(k \cdot p_\mu)} - \frac{p_e \cdot \bar{p}_\mu}{(k \cdot p_e)} \right) (k^\alpha \bar{p}_e^\beta + k^\beta \bar{p}_e^\alpha - k \cdot \bar{p}_e g^{\alpha\beta}) \\
&+ \frac{k \cdot \bar{p}_e}{(k \cdot p_e)^2} (p_e^\alpha \bar{p}_\mu^\beta + p_e^\beta \bar{p}_\mu^\alpha - p_e \cdot \bar{p}_\mu g^{\alpha\beta}) - \frac{k \cdot \bar{p}_\mu}{(k \cdot p_\mu)^2} (p_\mu^\alpha \bar{p}_e^\beta + p_\mu^\beta \bar{p}_e^\alpha - p_\mu \cdot \bar{p}_e g^{\alpha\beta}) \\
&+ \left. \frac{k \cdot \bar{p}_\mu}{(k \cdot p_e)(k \cdot p_\mu)} (p_e^\alpha \bar{p}_e^\beta + p_e^\beta \bar{p}_e^\alpha - m_e^2 g^{\alpha\beta}) - \frac{k \cdot \bar{p}_e}{(k \cdot p_e)(k \cdot p_\mu)} (p_\mu^\alpha \bar{p}_\mu^\beta + p_\mu^\beta \bar{p}_\mu^\alpha - m_\mu^2 g^{\alpha\beta}) \right\} \\
&- \frac{e^2}{2} \left( \bar{p}_e^\alpha \bar{p}_\mu^\beta + \bar{p}_e^\beta \bar{p}_\mu^\alpha - \bar{p}_e \cdot \bar{p}_\mu g^{\alpha\beta} \right) \left( \frac{m_\mu^2}{(k \cdot p_\mu)^2} + \frac{m_e^2}{(k \cdot p_e)^2} - 2 \frac{p_e \cdot p_\mu}{(k \cdot p_e)(k \cdot p_\mu)} \right). \quad (29)
\end{aligned}$$

In the last line of Eq. (29) we have isolated the infrared singular piece of the charge-side tensor which is given by the usual soft photon factor multiplying the Born term contribution. In the phase space integration over the photon momentum the infrared singular piece is regularized by introducing a (small) photon mass which distorts the phase space away from the singular point. The infrared singular piece is cancelled by the corresponding singular piece in the one-loop contributions again calculated in Feynman gauge. In the one-loop amplitude the photon mass is included in the pole denominators only<sup>7</sup>.

The remaining part of the charge-side tensor in Eq. (29) is infrared finite and can easily be integrated without a regulator photon mass.

Just as in the Born term case treated in Sec. 3 the  $O(\alpha)$  charge-side tensor  $C_{\alpha\beta}^{(\alpha)}$  is contracted with the neutral-side tensor  $N^{\alpha\beta}$  Eq. (16) where now  $Q = p_\mu - p_e - k$ . One then performs the appropriate tree graph integrations over the photon's momentum and adds in the one-loop contributions. The final result is

$$\begin{aligned}
G_1^{(\alpha)} &= \frac{\alpha}{\pi} G_1^{Born} \Sigma + \frac{\alpha}{\pi} \frac{1}{12\beta x} \left\{ 3\beta x \left( (3 - 4x)x - (8 - 9x)y^2 \right) \lambda_1 \right. \\
&+ \left. \left( (5 + 12x - 51x^2 + 28x^3) - 3(19 - 40x + 17x^2)y^2 - 3(19 - 4x)y^4 + 5y^6 \right) \lambda_2 \right.
\end{aligned}$$

---

<sup>7</sup>We specify our infrared regularization procedure since, historically, there has been a certain amount of controversy concerning the use of a photon mass regulator (see e.g. [19]).

$$- 4\beta x \left( (11 - 10x + 5x^2) - 2(1 + 5x)y^2 + 11y^4 \right) \Big\}, \quad (30)$$

$$\begin{aligned} G_2^{(\alpha)} &= \frac{\alpha}{\pi} G_2^{Born} \Sigma + \frac{\alpha}{\pi} \frac{1}{12\beta^2 x^2} \left\{ 3\beta^3 x^3 (1 - 4x + 9y^2) \lambda_1 - 8(1 - x + y^2)^3 \lambda_3 \right. \\ &\quad - \left( x(1 + 33x^2 - 28x^3) - 3x(33 - 12x - 17x^2)y^2 + 3(32 - 35x - 4x^2)y^4 - 5xy^6 \right) \lambda_2 \\ &\quad \left. - 2\beta x \left( (3 - 10x - 13x^2 + 8x^3) + (59 - 11x^2)y^2 - (35 - 10x)y^4 + 5y^6 \right) \right\}, \quad (31) \end{aligned}$$

$$\begin{aligned} G_3^{(\alpha)} &= \frac{\alpha}{\pi} G_3^{Born} \Sigma + \frac{\alpha}{\pi} \frac{1}{12\beta^2 x^2} \left\{ - 3\beta^3 x^3 (3 - 4x + 3y^2) \lambda_1 - 8y^2 (1 - x + y^2)^3 \lambda_3 \right. \\ &\quad - \left( x(5 + 12x - 51x^2 + 28x^3) - (8 - 129x + 60x^2 + 25x^3)y^2 \right. \\ &\quad \left. - 3(40 - 49x + 8x^2)y^4 - (24 - 23x)y^6 - 8y^8 \right) \lambda_2 \\ &\quad \left. + 2\beta x \left( (5 + 10x - 11x^2 + 8x^3) - (35 + 13x^2)y^2 + (59 - 10x)y^4 + 3y^6 \right) \right\}, \quad (32) \end{aligned}$$

$$\begin{aligned} G_4^{(\alpha)} &= \frac{\alpha}{\pi} G_4^{Born} \Sigma + \frac{\alpha}{\pi} \frac{1}{12\beta^3 x^3} \left\{ - 3\beta^3 x^3 \left( (1 - 4x)x + (8 + 3x)y^2 \right) \lambda_1 \right. \\ &\quad + 8x(1 - y^2)(1 - x + y^2)^3 \lambda_3 + 4\beta x \left( x(1 - 5x - 5x^2 + 3x^3) \right. \\ &\quad - (4 - 59x + 14x^2 + 5x^3)y^2 - (104 - 59x + 5x^2)y^4 - (4 - x)y^6 \Big) \\ &\quad + \left( x^2(1 + 33x^2 - 28x^3) + (4 + 8x - 153x^2 + 104x^3 + 25x^4)y^2 \right. \\ &\quad \left. - 3(28 - 72x + 59x^2 - 8x^3)y^4 - (84 - 24x + 23x^2)y^6 + 4(1 + 2x)y^8 \right) \lambda_2 \Big\} \quad (33) \end{aligned}$$

$$G_5^{(\alpha)} = \frac{\alpha}{\pi} G_5^{Born} \Sigma + \frac{\alpha y}{\pi 2} \left\{ - (1 - 2x + 3y^2) \lambda_1 + \frac{2}{\beta x} (3x - 2x^2 - (4 - 3x)y^2) \lambda_2 \right\}. \quad (34)$$

We have used the abbreviations

$$\lambda_1 = \ln y^2, \quad \lambda_2 = \ln \left( \frac{1 + \beta}{1 - \beta} \right), \quad \lambda_3 = \ln \left( \frac{2 - (1 + \beta)x}{2 - (1 - \beta)x} \right) \quad (35)$$

and

$$\begin{aligned} \Sigma &= \frac{1}{\beta} \left\{ 2\text{Li}_2\left(\frac{2\beta x}{2 - (1 - \beta)x}\right) - 2\text{Li}_2\left(\frac{2\beta x}{(1 + \beta)x - 2y^2}\right) - \beta \ln(1 - x + y^2) \right. \\ &\quad \left. + \left( \ln\left((1 + \beta)\frac{x}{2}\right) - \frac{1 - y^2}{x} \right) (\lambda_3 - \lambda_2) + \left( \ln\left(1 - (1 + \beta)\frac{x}{2}\right) - \frac{1 - x}{x} \right) \lambda_2 \right\}. \end{aligned} \quad (36)$$

Our results for  $G_1^{(\alpha)}$  and  $G_2^{(\alpha)}$  agree with those of [7]. Note that the four spectrum functions  $G_{1,2,3,4}^{(\alpha)}$  are logarithmically mass divergent. We have checked that the expansion of the spectrum functions  $G_{1,2,3,4}^{(\alpha)}$  and  $G_5^{(\alpha)}/y$  in terms of powers of  $y$  contains only even powers of  $y$ , in agreement with the general reasoning given in [15]. The leading term in the  $y$ -expansion of the spectrum functions  $G_{1,2,3,4}^{(\alpha)}$  can be reconstructed from the  $m_e \rightarrow 0$  results to be presented in Sec. 6. We do not write down any of the higher order coefficients in the  $y$ -expansion, as was done in the Born term case, since such an expansion is not particularly illuminating.

In Fig. 2a ( $\mu \rightarrow e$ ), Fig. 3a ( $\tau \rightarrow \mu$ ) and Fig. 4a ( $\tau \rightarrow e$ ) we show plots of the  $x$ -dependence of the four spectrum functions  $\beta x G_i$  ( $i = 1, 2, 3, 4$ ), with and without radiative corrections. The radiative corrections show a marked  $y$ -dependence. They are smallest for  $\tau \rightarrow \mu$ , become larger for  $\mu \rightarrow e$ , and are largest for  $\tau \rightarrow e$ . To a large part this can be traced to the  $(\ln y)$ -dependent terms in the spectrum functions as will be discussed in more detail in Sec. 6. On an *absolute* scale the radiative corrections are generally quite small except for the hard end of the spectrum where they in fact (logarithmically) diverge<sup>8</sup>. On a *relative* scale the radiative corrections are quite large for ( $\mu \rightarrow e$ ) and for ( $\tau \rightarrow e$ ), and smaller for ( $\tau \rightarrow \mu$ ) at the soft end of the spectrum, where the spectrum functions are small. This will show up in the radiative corrections to the longitudinal polarization of the daughter lepton  $P_V^l$  and the forward-backward asymmetry  $A_{FB}$  which are large in the threshold region for  $\mu \rightarrow e$  and  $\tau \rightarrow e$  and small for  $\tau \rightarrow \mu$ . As discussed in Sec. 3 the contribution of  $\beta x G_5$  is barely discernible for the case  $\tau \rightarrow \mu$  (Fig. 3a). At the scale of the figure the difference between the Born and NLO curves is not visible.

It is interesting to note that the radiative corrections go through zeros close to  $x = 0.68$  and  $x = 0.82$  for  $G_{1,3}$  and for  $G_{2,4}$ , respectively, for all three cases discussed in this paper. The positions of the respective zeros are practically mass independent. Differences in the position of the zero show up only in the third digit. In fact, when discussing the

---

<sup>8</sup>The divergent terms at the endpoint of the electron spectrum can be resummed into an exponential function [20, 21].

$m_\nu \rightarrow 0$  case in Sec. 6 we have checked that the positions of the zeroes remain practically unchanged even when letting  $y \rightarrow 0$ . The radiative corrections are negative and positive below and above the zero for  $\beta x G_{1,4}$ , resp., and positive and negative below and above the zero for  $\beta x G_{2,3}$ . Qualitatively the alternating sign pattern over the range of the spectrum can be understood from the dominance of the  $(\ln y)$ -terms and from the fact that the  $(\ln y)$ -dependent terms have to cancel out when one integrates over the spectrum. There is a tendency of the radiative corrections to cancel in the sums  $(G_1 + G_3)$  and  $(G_2 + G_4)$  and to add up in the differences  $(G_1 - G_3)$  and  $(G_2 - G_4)$ , i.e. the radiative corrections add destructively and constructively in the final electron's density matrix elements  $\rho_{++}$  and  $\rho_{--}$ , resp., to be discussed further in Sec. 6.

We next turn to the radiative corrections of the longitudinal polarization  $P_e^l$  of the electron and the forward-backward asymmetry  $A_{FB}$  calculated according to Eqs. (9) and (20). We begin by discussing the limiting value of the longitudinal polarization at the soft end of the spectrum including the radiative corrections. At NLO one has

$$\begin{aligned} \lim_{x \rightarrow 2y} P_e^l &= -\frac{1}{3} P \cos \theta_P \left\{ 1 - \frac{\alpha}{\pi} \frac{4(1-y)^2(1+y^2)}{72y^2 + \frac{\alpha}{\pi}(5-10y-278y^2-10y^3+5y^4) - 108\frac{\alpha}{\pi} \frac{1+y}{1-y} y^2 \ln y} \right\} \\ &\approx -\frac{1}{3} P \cos \theta_P \left\{ 1 - \frac{\alpha}{\pi} \left( 18y^2 + \frac{5\alpha}{4\pi} \right)^{-1} \right\}. \end{aligned} \quad (37)$$

For the cases  $\mu \rightarrow e$  and  $\tau \rightarrow e$  the term  $(18y^2)$  in the second line of Eq. (37) can be neglected and thus the limiting value of the longitudinal polarization of the electron is given by  $P_e^l \approx -\frac{1}{15} P \cos \theta_P$  which is smaller than the Born term value by a factor of 5. This is evident in Figs. 2b and 4b where the radiative corrections to the longitudinal polarization of the electron are shown. For the  $\tau \rightarrow \mu$  case the term  $(18y^2)$  dominates over  $(5/4)(\alpha/\pi)$  and the limiting value of the longitudinal polarization of the  $\mu$  is  $P_e^l \approx -\frac{1}{3} P \cos \theta_P (1 - \frac{\alpha}{\pi} \frac{1}{18y^2})$ , i.e. the correction to the Born term value is only  $\approx 3.6\%$ . This can be seen in Fig. 3b. The NLO limiting value for the forward-backward asymmetry is zero since after a Taylor series expansion one finds  $G_2^{(\alpha)}/G_1^{(\alpha)} \simeq (x - x_{min})^{1/2}$  just as in the Born term case. This can again be seen in Figs. 2c - 4c. Finally, the behaviour of the transverse polarization  $P_e^\perp$  at  $x_{min} = 2y$  is quite similar to that of the longitudinal polarization. In fact, one just has to replace  $\cos \theta_P \rightarrow \sin \theta_P$  and  $4 \rightarrow 5$  in the numerator of the first line of Eq.(37) in order to obtain the limiting value  $P_e^\perp$ . This leads to

$$\lim_{x \rightarrow 2y} P_e^\perp \approx -\frac{1}{3} P \sin \theta_P \left\{ 1 - \frac{\alpha}{\pi} \left( \frac{72}{5} y^2 + \frac{\alpha}{\pi} \right)^{-1} \right\}. \quad (38)$$

Just as for  $P_e^l$  the  $O(\alpha)$  corrections are small for  $\tau \rightarrow \mu$  and sizeable for  $\mu \rightarrow e$  and  $\tau \rightarrow e$  at threshold, as can be seen in Figs. 2b - 4b. Next we discuss the limiting behaviour of the spectrum functions at the hard end of the spectrum, where  $x \rightarrow x_{max} = 1 + y^2$ . As remarked on before the radiative correction contributions can be seen to logarithmically diverge in this limit (see footnote 7). Introducing  $x'_{max} = 1 + y^2 - \varepsilon$  the limiting behaviour of the four spectrum functions is given by

$$\lim_{x \rightarrow x_{max}} G_1 = - \lim_{x \rightarrow x_{max}} G_2 = - \lim_{x \rightarrow x_{max}} G_3 = \lim_{x \rightarrow x_{max}} G_4 = (1 - y^2)^2 + \frac{\alpha}{\pi} 2(1 - y^2) \times \quad (39)$$

$$\times \left\{ (1 + y^2) \left( \frac{3}{4} + \ln \left( \frac{\varepsilon}{1 - y^2} \right) \right) \ln y + (1 - y^2) \left( 1 + \ln \left( \frac{\varepsilon}{1 - y^2} \right) \right) \right\}.$$

The limiting values of the four spectrum functions are, up to signs, all identical. This implies that the radiative corrections to the longitudinal polarization of the daughter lepton does not change the Born term value  $P_{l'}^l = -1$  at the hard end of the spectrum irrespective of the values of  $P \cos \theta_P$ . Similarly the radiative corrections to the forward-backward asymmetry do not change the Born term value of  $A_{FB} = -\frac{1}{2}P$  at the hard end of the spectrum. Finally, the NLO transverse polarization is zero at  $x = x_{max}$  since  $G_5^{(\alpha)}$  is finite at  $x_{max}$ . In fact, one has  $G_5^{(\alpha)} \rightarrow -(\alpha/\pi)y(1 - y^2) \ln y$  at  $x_{max}$ .

The fact that the relative corrections to the spectrum functions in the threshold region are *relatively* large for  $(\mu \rightarrow e)$  and  $(\tau \rightarrow e)$  shows up in Figs. 2b and 4b, and in Figs. 2c and 4c, where the radiative corrections to the longitudinal polarization of the final state electrons and the forward-backward asymmetry are visibly large in the threshold region<sup>9</sup>. Note, though, that we have enhanced the threshold region in our presentation of  $P_{l'}^l$  and  $A_{FB}$  by choosing a logarithmic scale for  $x$  in Figs. 2b,c, 3b,c and 4b,c. For the forward-backward asymmetry the radiative corrections remain large over a larger part of the spectrum. The radiative corrections to  $P_{\mu}^l$  and  $A_{FB}$  for the  $(\tau \rightarrow \mu)$  decays are shown in Figs. 3b and 3c. As expected from the smallness of the radiative corrections to the spectrum functions shown in Fig. 3a the radiative corrections to both the longitudinal polarization of the final state muon and the forward-backward asymmetry are small. The same statement holds true for the radiative corrections to the transverse polarization. Since the spectrum functions are small at the soft end of the spectrum, the radiatively corrected average longitudinal polarization  $\langle P_{l'}^l \rangle$  of the daughter lepton  $l'$  is expected to

---

<sup>9</sup>In our numerical results for the longitudinal and transverse polarization of the daughter lepton and the forward-backward asymmetry we have *not* expanded out the inverse of the denominator function in terms of powers of  $\alpha$ .

remain very close to  $-1$  in all three cases. Using the integrated rate functions presented at the end of this section we find the NLO result  $\langle P_V^l \rangle = -0.999, -0.986$  and  $-0.999$  for  $(\mu \rightarrow e)$ ,  $(\tau \rightarrow \mu)$  and  $(\tau \rightarrow e)$ , resp., for  $\cos \theta_P = 0$  with very little dependence on  $\cos \theta_P$ . The corresponding figures for  $\langle A_{FB} \rangle$  are  $-0.166, -0.170, -0.166$ . Finally, for the transverse polarization one finds  $\langle P_V^\perp \rangle = -0.0031, -0.037, -0.00018$  for the three cases for  $\cos \theta_P = 0$ .

Next we integrate the five spectrum functions  $\beta x G_i^{(\alpha)}$  over the electron spectrum according to (22). One obtains

$$\begin{aligned}
\hat{G}_1^{(\alpha)} = & \frac{\alpha}{\pi} \left\{ \frac{1}{48} (1 - y^4) (75 - 956y^2 + 75y^4) - y^4 (36 + y^4) \ln^2 y \right. \\
& - \frac{\pi^2}{4} (1 - 32y^3 + 16y^4 - 32y^5 + y^8) - \frac{1}{6} (60 + 270y^2 - 4y^4 + 17y^6) y^2 \ln y \\
& - \frac{1}{12} (1 - y^4) (17 - 64y^2 + 17y^4) \ln(1 - y^2) \\
& + 2(1 - y)^4 (1 + 4y + 10y^2 + 4y^3 + y^4) \ln(1 - y) \ln y \\
& + 2(1 + y)^4 (1 - 4y + 10y^2 - 4y^3 + y^4) \ln(1 + y) \ln y \\
& + (3 + 32y^3 + 48y^4 + 32y^5 + 3y^8) \text{Li}_2(-y) \\
& \left. + (3 - 32y^3 + 48y^4 - 32y^5 + 3y^8) \text{Li}_2(y) \right\}, \tag{40}
\end{aligned}$$

$$\begin{aligned}
\hat{G}_2^{(\alpha)} = & \frac{\alpha}{\pi} \left\{ \frac{1}{3} (1 - y^2) (1 + y^2 + 13y^4 - 3y^6) (\ln(1 - y) + 2 \ln(1 + y)) \ln y \right. \\
& - \frac{1}{432} (1 - y)^2 (617 - 842y + 1929y^2 - 1592y^3 - 3415y^4 + 54y^5 - 567y^6) \\
& - \frac{1}{36} (1 - y) y (12 - 18y - 238y^2 + 41y^3 - 1003y^4 - 45y^5 - 9y^6) \ln y \\
& \left. + \frac{1}{36} (1 - y)^2 (13 + 26y + 87y^2 - 364y^3 + 535y^4 - 102y^5 - 51y^6) \ln(1 - y) \right\}
\end{aligned}$$

$$\begin{aligned}
& + \frac{1}{2}y^4(14 + 32y^2 - 3y^4) \ln^2 y - \frac{1}{9}(1 - y^2)(25 + 13y^2 + 67y^4 + 15y^6) \ln(1 + y) \\
& - 8y^4 \left( \frac{1}{6} \ln^3 y + \left( 2\text{Li}_2(-y) + \text{Li}_2(y) - \frac{\pi^2}{3} \right) \ln y - 6\text{Li}_3(-y) - \text{Li}_3(y) - \frac{7}{2}\zeta(3) \right) \\
& + \frac{1}{3}(7 + 24y^2 + 48y^4 - 8y^6 + 9y^8) \left( \text{Li}_2(-y) + \frac{\pi^2}{12} \right) \Big\}, \tag{41}
\end{aligned}$$

$$\begin{aligned}
\hat{G}_3^{(\alpha)} &= \frac{\alpha}{\pi} \left\{ \frac{1}{3}(1 - y^2)(3 - 13y^2 - y^4 - y^6)(\ln(1 - y) + 2 \ln(1 + y)) \ln y \right. \\
& - \frac{1}{432}(1 - y)^2(567 - 54y + 3415y^2 + 1592y^3 - 1929y^4 + 842y^5 - 617y^6) \\
& - \frac{1}{36}(1 - y)y(36 + 98y + 590y^2 - 265y^3 + 27y^4 - 99y^5 - 87y^6) \ln y \\
& + \frac{1}{36}(1 - y)^2(51 + 102y - 535y^2 + 364y^3 - 87y^4 - 26y^5 - 13y^6) \ln(1 - y) \\
& - \frac{1}{6}y^2(8 + 66y^2 - 24y^4 - y^6) \ln^2 y - \frac{1}{9}(1 - y^2)(15 + 67y^2 + 13y^4 + 25y^6) \ln(1 + y) \\
& + 8y^4 \left( \frac{1}{6} \ln^3 y + \left( 2\text{Li}_2(-y) + \text{Li}_2(y) - \frac{\pi^2}{3} \right) \ln y - 6\text{Li}_3(-y) - \text{Li}_3(y) - \frac{7}{2}\zeta(3) \right) \\
& \left. + \frac{1}{3}(9 - 8y^2 + 48y^4 + 24y^6 + 7y^8) \left( \text{Li}_2(-y) + \frac{\pi^2}{12} \right) \right\}, \tag{42}
\end{aligned}$$

$$\begin{aligned}
\hat{G}_4^{(\alpha)} &= \frac{\alpha}{\pi} \left\{ \frac{1}{432}(1 - y^4)(581 + 6140y^2 + 581y^4) \right. \\
& - \frac{\pi^2}{36}(7 - 6y + 28y^2 + 222y^3 - 164y^4 + 390y^5 - 140y^6 + 66y^7 - 5y^8) \\
& - \frac{1}{36}(1 - y^4)(13 - 176y^2 + 13y^4) \ln(1 - y^2) + \frac{1}{3}y^2(2 + 46y^2 + 38y^4 + y^6) \ln^2 y \\
& + \frac{2}{3}y(1 - y)^4(5 - 4y + 5y^2) \ln(1 - y) \ln y - \frac{2}{3}y(1 + y)^4(5 + 4y + 5y^2) \ln(1 + y) \ln y \\
& \left. + \frac{1}{18}y^2(212 + 930y^2 + 388y^4 - 13y^6) \ln y \right\}
\end{aligned}$$

$$\begin{aligned}
& + \frac{1}{3}(1 - 10y - 56y^2 - 102y^3 - 164y^4 - 102y^5 - 56y^6 - 10y^7 + y^8)\text{Li}_2(-y) \\
& + \frac{1}{3}(1 + 10y - 56y^2 + 102y^3 - 164y^4 + 102y^5 - 56y^6 + 10y^7 + y^8)\text{Li}_2(y) \Big\}, \quad (43)
\end{aligned}$$

$$\begin{aligned}
\hat{G}_5^{(\alpha)} = & \frac{\alpha}{\pi} y \Big\{ - \frac{7}{18}(1 - y^2)(5 + 34y^2 + 5y^4) \\
& - \frac{2}{3}y^2(9 + 18y^2 - y^4)\ln^2 y + \frac{\pi^2}{6}(1 - 3y^2 + 32y^3 - 3y^4 + y^6) \\
& - \frac{4}{3}(1 - y)^4(1 + 4y + y^2)\ln(1 - y)\ln y - \frac{4}{3}(1 + y)^4(1 - 4y + y^2)\ln(1 + y)\ln y \\
& - \frac{1}{18}(15 + 249y^2 + 141y^4 - 29y^6)\ln y + \frac{1}{9}(1 - y^2)(11 + 38y^2 + 11y^4)\ln(1 - y^2) \\
& - \frac{2}{3}(3 - 9y^2 - 32y^3 - 9y^4 + 3y^6)\text{Li}_2(-y) \\
& - \frac{2}{3}(3 - 9y^2 + 32y^3 - 9y^4 + 3y^6)\text{Li}_2(y) \Big\}. \quad (44)
\end{aligned}$$

Note that  $\hat{G}_2^{(\alpha)}$  and  $\hat{G}_3^{(\alpha)}$  contain trilog functions, and associated with them, Euler's *Zeta* function  $\zeta(3)$ , whereas  $\hat{G}_1^{(\alpha)}$ ,  $\hat{G}_4^{(\alpha)}$  and  $\hat{G}_5^{(\alpha)}$  contain only dilog functions. In agreement with the Lee–Nauenberg theorem [3] the rate functions do not contain any logarithmic mass singularities. Our result for  $\hat{G}_1^{(\alpha)}$  agrees with the result in [22] where a different route of phase space integrations was taken to arrive at the total rate. Our result for  $\hat{G}_2^{(\alpha)}$  agrees with the result in [7]. The results on  $\hat{G}_3^{(\alpha)}$ ,  $\hat{G}_4^{(\alpha)}$  and  $\hat{G}_5^{(\alpha)}$  are new. As an additional check we have checked that all five rate functions  $\hat{G}_i^{(\alpha)}$  vanish for  $y \rightarrow 1$ .

In order to get a quantitative feeling about the size of the radiative corrections to the respective spectrum functions we have listed in Tab. 2 the percentage changes  $\delta\hat{G}_i$  induced by the radiative corrections, where

$$\delta\hat{G}_i = \frac{(\hat{G}_i^{(\alpha)} + \hat{G}_i^{Born}) - \hat{G}_i^{Born}}{\hat{G}_i^{Born}} = \frac{\hat{G}_i^{(\alpha)}}{\hat{G}_i^{Born}}. \quad (45)$$

The relative radiative corrections  $\delta\hat{G}_i$  can all be seen to be close to the naive expectation of  $O(\alpha)$  where the relative radiative corrections to  $\hat{G}_5$  are largest. However, as was emphasized earlier on, all radiative corrections discussed in this paper go through zeros.

$i$	$\mu \rightarrow e$			$\tau \rightarrow \mu$			$\tau \rightarrow e$		
	$\delta\hat{G}_i^<$	$\delta\hat{G}_i^>$	$\delta\hat{G}_i$	$\delta\hat{G}_i^<$	$\delta\hat{G}_i^>$	$\delta\hat{G}_i$	$\delta\hat{G}_i^<$	$\delta\hat{G}_i^>$	$\delta\hat{G}_i$
1	+2.80%	-2.69%	-0.42%	+0.76%	-1.14%	-0.40%	+ 5.20%	-4.44%	-0.42%
2	+8.22%	-3.70%	-0.68%	+2.51%	-1.59%	-0.62%	+14.70%	-6.10%	-0.68%
3	+2.56%	-2.68%	-0.53%	+0.66%	-1.14%	-0.45%	+ 4.95%	-4.43%	-0.54%
4	+7.82%	-3.70%	-0.79%	+2.53%	-1.59%	-0.67%	+14.28%	-6.10%	-0.80%
5	+0.76%	-3.68%	-2.89%	+0.09%	-1.62%	-1.49%	+ 1.72%	-6.03%	-4.53%

**Table 2:**

Numerical values of partially integrated ( $\delta\hat{G}_i^<$ ,  $\delta\hat{G}_i^>$ ) and total rate functions ( $\delta\hat{G}_i$ ) divided by their respective Born term values. The symbols “<” and “>” stand for integrations from threshold to the zero point of the respective  $O(\alpha)$  contributions, and from the zero point to the endpoint of the spectrum.

Integrating over the whole spectrum therefore does not give an adequate representation of the size of the radiative corrections to the spectrum since there are sizable cancellation effects. This cancellation would become less effective if moments of the spectrum functions were taken. The moments could be chosen such that they either emphasize the threshold or the endpoint region. Alternatively, one can consider partially integrated rates where the integrations either run from threshold to the point where the radiative corrections go to zero or from the zero point to the endpoint. The two partially integrated rate functions will be denoted by  $\hat{G}_i^<$  (lower part) and by  $\hat{G}_i^>$  (upper part). The two respective partially integrated relative rate functions  $\delta\hat{G}_i^<$  and  $\delta\hat{G}_i^>$  are also listed in Tab. 2. The relative radiative corrections for the partially integrated rate functions can be seen to be much larger than for the fully integrated rate functions and can amount up to  $O(10\%)$  which is much larger than the naive  $O(\alpha)$  expectation. Note, though, that, in contrast to the rate functions, neither the moments of the spectral functions nor the partially integrated rates are free of logarithmic mass singularities.

Since the complete rate expressions are rather unwieldy it is useful to consider the small  $y$ -expansions of the rate expressions. One has

$$\hat{G}_1^{(\alpha)} = \frac{\alpha}{\pi} \left\{ \frac{25 - 4\pi^2}{16} - (17 + 12 \ln y)y^2 + 8\pi^2 y^3 + O(y^4) \right\}, \quad (46)$$

$$\hat{G}_2^{(\alpha)} = \frac{\alpha}{\pi} \left\{ -\frac{617 - 84\pi^2}{432} - \frac{2}{3}y - \frac{1}{3}(24 - 2\pi^2 - \ln y)y^2 + \right. \\ \left. + \frac{2}{27}(71 + 84 \ln y)y^3 + O(y^4) \right\}, \quad (47)$$

$$\hat{G}_3^{(\alpha)} = \frac{\alpha}{\pi} \left\{ -\frac{21 - 4\pi^2}{16} - \frac{10}{3}y - \frac{1}{27}(232 + 6\pi^2 + 87 \ln y + \right. \\ \left. + 36 \ln^2 y)y^2 + \frac{2}{9}(121 - 84 \ln y)y^3 + O(y^4) \right\}, \quad (48)$$

$$\hat{G}_4^{(\alpha)} = \frac{\alpha}{\pi} \left\{ \frac{7(83 - 12\pi^2)}{432} + \frac{1}{6}y + \frac{1}{27}(578 - 21\pi^2 + 138 \ln y + \right. \\ \left. + 18 \ln^2 y)y^2 - \frac{37}{6}\pi^2 y^3 + O(y^4) \right\}, \quad (49)$$

$$\hat{G}_5^{(\alpha)} = \frac{\alpha}{\pi} y \left\{ -\frac{35 - 3\pi^2 + 15 \ln y}{18} - \frac{1}{2}(27 + \pi^2 + 25 \ln y + \right. \\ \left. + 12 \ln^2 y)y^2 + \frac{16}{3}\pi^2 y^3 + O(y^4) \right\}. \quad (50)$$

It is well-known that the  $O(\alpha)$  small- $y$  corrections to the reduced rate  $\hat{G}_1^{(\alpha)}$  start only at  $O(y^2)$  (see e.g. [15, 23]). In contradistinction and contrary to the Born term case the mass corrections to the spin dependent rate functions  $\hat{G}_2^{(\alpha)}$ ,  $\hat{G}_3^{(\alpha)}$  and  $\hat{G}_4^{(\alpha)}$  all start at  $O(y)$ .

In order to obtain a quantitative feeling about the importance of mass effects in the  $O(\alpha)$  radiative contributions we have listed in Tab. 1 the percentage changes in the rate functions  $\hat{G}_i$  when going from  $m_{l'} \rightarrow 0$  to  $m_{l'} \neq 0$  using the  $m_{l'} \rightarrow 0$  results listed in Sec. 6. The mass effects are not small, in particular for the case ( $\tau \rightarrow \mu$ ). The percentage changes for the radiative contributions are larger than those in the Born term case which is partly due to the difference in the power pattern of the final state lepton mass corrections in the two cases. The quality of the  $m_{l'} \rightarrow 0$  approximation for the radiative corrections can be assessed by referring again to Tab. 1. The final state lepton mass effects tend to reduce the overall size of the radiative corrections. The reduction is largest ( $O(10\%)$ ) for the case ( $\tau \rightarrow \mu$ ) and smallest ( $O(10^{-1})$ ) for the case ( $\tau \rightarrow e$ ). They are largest for the rate functions  $\hat{G}_3$  and  $\hat{G}_4$  and smallest for  $\hat{G}_1$ . That the mass effects are smallest for  $\hat{G}_1$  is due

to the fact that the mass corrections to  $\hat{G}_1$  set in only at  $O(y^2)$  (see Eq. (47)). Whether one is willing to tolerate the error incurred in using the simpler  $m_{l'} \rightarrow 0$  radiative correction formulas depends of course on the accuracy required for the application at hand.

We now turn to the discussion of the NLO average longitudinal and transverse polarization of the electron  $\langle P_e^l \rangle$  and  $\langle P_e^\perp \rangle$ , and the NLO average forward–backward asymmetry  $\langle A_{FB} \rangle$ . They take remarkably simple forms in the  $y \rightarrow 0$  limit. Including the Born term contribution and expanding the inverse denominator in powers of  $\alpha/\pi$  one has at NLO

$$\lim_{y \rightarrow 0} \langle P_e^l \rangle = -\left(1 - \frac{\alpha}{2\pi}\right). \quad (51)$$

Note that  $\langle P_e^l \rangle$  does not depend on  $P \cos \theta_P$  in this approximation. For the forward–backward asymmetry one obtains

$$\lim_{y \rightarrow 0} \langle A_{FB} \rangle = -\frac{1}{6}P \left(1 - \frac{\alpha}{\pi} \frac{6\pi^2 - 49}{9}\right). \quad (52)$$

Finally, for the transverse polarization one obtains in the same approximation ( $\cos \theta = 0$ )

$$\lim_{y \rightarrow 0} \langle P_e^\perp \rangle = -\frac{2}{3}P y \left(1 + \frac{\alpha}{\pi} \frac{65 + 60 \ln y}{24}\right). \quad (53)$$

The  $O(\alpha)$  corrections to  $\langle P_e^l \rangle$ ,  $\langle A_{FB} \rangle$  and to  $\langle P_e^\perp \rangle$  are thus quite small. The actual numerical values for  $\langle P_e^l \rangle$ ,  $\langle A_{FB} \rangle$  and for  $\langle P_e^\perp \rangle$  listed earlier in this section lie very close to the above estimates in all three cases.

## 6 The $m_e \rightarrow 0$ limit and the anomalous helicity flip contribution

The purpose of this section is two-fold. First we discuss the  $m_e \rightarrow 0$  limit of the  $m_e \neq 0$   $O(\alpha)$  results given in Sec. 5. This allows us to make contact with the  $m_e \rightarrow 0$  results derived previously [6]. Second we discuss in some detail the origin of the anomalous helicity flip contribution resulting from collinear photon emission of the electron. Our results are presented in terms of the two diagonal components of the density matrix of the final state electron, which, in the limit  $m_e \rightarrow 0$ , are nothing but the helicity no–flip and helicity flip contributions of the final state electron. The naive prediction of massless QED is that the helicity flip contributions vanish in all orders of perturbation theory. However, as first pointed out by Lee and Nauenberg [3], there will be a nonzero helicity flip contribution from collinear photon emission which survives the  $m_e \rightarrow 0$  limit. This will be demonstrated in our  $O(\alpha)$   $m_e \rightarrow 0$  expressions. Our  $m_e \rightarrow 0$  result for the helicity

flip contribution is found to be in agreement with expectations derived from the universal equivalent particle approach of Falk and Sehgal [5]. For a discussion of the quality of the  $m_{\nu} \rightarrow 0$  approximation for the three cases ( $\mu \rightarrow e$ ), ( $\tau \rightarrow \mu$ ) and ( $\tau \rightarrow e$ ) we refer to the discussion at the end of Sec. 5.

Since we want to discuss the helicity no-flip and flip contributions separately it is convenient to choose a slightly different representation for the differential rate Eq. (6). We write the differential rate in terms of the no-flip and flip contributions

$$\frac{d\Gamma}{dx d\cos\theta_P} = \frac{d\Gamma^{nf}}{dx d\cos\theta_P}(1 - \cos\theta) + \frac{d\Gamma^{hf}}{dx d\cos\theta_P}(1 + \cos\theta), \quad (54)$$

where the no-flip and flip contributions are given by

$$\frac{d\Gamma^{nf/hf}}{dx d\cos\theta_P} = \frac{1}{2}\beta x \Gamma_0 \left( (G_1 \mp G_3) + (G_2 \mp G_4)P \cos\theta_P \right). \quad (55)$$

The terminology helicity no-flip ( $nf$ ) and helicity flip ( $hf$ ) is really only appropriate in the  $m_e \rightarrow 0$  limit where the electron emerging from the left-chiral weak interaction current is purely left-handed. After photon emission the electron can then remain left-handed ( $nf$ ) or can become right-handed ( $hf$ ). For  $m_e \neq 0$  the respective  $nf$  and  $hf$  contributions are nothing but the (unnormalized) diagonal elements of the density matrix of the electron, i.e.  $\Gamma^{nf} \sim \rho_{--}$  and  $\Gamma^{hf} \sim \rho_{++}$ .

As concerns the helicity flip contribution one notes that there are no Born term helicity flip contributions in the limit  $m_e = 0$  since a massless electron emerging from the weak ( $V - A$ ) vertex is left-handed. This is explicitly seen by inserting the Born term rate functions Eq. (19) in Eq. (55). Naively, one would expect no helicity flip contributions also at  $O(\alpha)$  because, in massless QED with  $m_e = 0$ , photon emission from the electron is helicity conserving. However, taking the limit  $m_e \rightarrow 0$  in Eqs. (30) - (33) one finds helicity flip contributions which survive the  $m_e \rightarrow 0$  limit. In fact, one finds

$$\frac{d\Gamma^{hf}}{dx d\cos\theta_P} = \frac{\alpha}{12\pi} \Gamma_0 \left( \left[ (1-x)^2(5-2x) \right] - \left[ (1-x)^2(1+2x) \right] P \cos\theta_P \right), \quad (56)$$

which agrees with the result presented in Ref. [6]. Because of the naive expectation that the helicity flip contribution vanishes in massless QED the presence of a helicity flip contribution is sometimes referred to as the anomalous helicity flip contribution. Moreover, the authors of Ref. [24] were able to show that the well-known axial anomaly can be traced to the existence of an anomalous helicity flip contribution to the absorptive part of the  $VVA$  triangle diagram in massless QED. This gives further justification for the use of the terminology ‘‘anomalous helicity flip contribution’’. In order to set the

anomalous contributions apart we have highlighted them in Eq. (56) by enclosing them in square brackets.

The authors of Ref. [6] had already expressed surprise at the simplicity of the structure of the  $O(\alpha)$  helicity flip contributions without, however, attempting to identify the source of this structural simplicity. The simplicity of the helicity flip contribution becomes manifest in the equivalent particle description of  $\mu$ -decay where, in the peaking approximation,  $\mu$ -decay is described by the two-stage process  $\mu^- \rightarrow e^-$  followed by the branching process  $e^- \rightarrow e^- + \gamma$  characterized by universal splitting functions  $D_{nf/hf}(z)$  [5]. In the splitting process  $z$  is the fractional energy of the emitted photon [5]. The off-shell electron in the propagator is replaced by an equivalent on-shell electron in the intermediate state. Since the helicity flip contribution arises entirely from the collinear configuration it can be calculated in its entirety using the equivalent particle description.

The helicity flip splitting function is given by  $D_{hf}(z) = \alpha z / (2\pi)$ , where  $z = k_0 / E' = (E' - E) / E' = 1 - x / x'$ , and where  $k_0$  is the energy of the emitted photon [5].  $E'$  and  $E$  denote the energies of the initial and final electron in the splitting process. The helicity flip splitting function has to be folded with the appropriate  $m_e = 0$  Born term contribution. The lower limit of the folding integration is determined by the soft photon point where  $E' = E$ . The upper limit is determined by the maximal energy of the initial electron  $E' = m_\mu / 2$ . One obtains

$$\begin{aligned} \frac{d\Gamma^{hf}}{dx d\cos\theta_P} &= \frac{\alpha}{2\pi} \int_x^1 dx' \frac{1}{x'} \frac{d\Gamma^{Born;nf}(x')}{dx' d\cos\theta_P} \left(1 - \frac{x}{x'}\right) \\ &= \frac{\alpha}{2\pi} \Gamma_0 \int_x^1 dx' (x' - x) \left( (3 - 2x') + (1 - 2x') P \cos\theta_P \right) \\ &= \frac{\alpha}{12\pi} \Gamma_0 \left( (1 - x)^2 (5 - 2x) - (1 - x)^2 (1 + 2x) P \cos\theta_P \right), \end{aligned} \quad (57)$$

which exactly reproduces the result of Eq. (56). Note that the flip spectrum function does not contain a logarithmic mass factor. Integrating over the spectrum one obtains

$$\frac{d\langle\Gamma^{hf}\rangle}{d\cos\theta_P} = \frac{\alpha}{\pi} \Gamma_0 \left( \left[ \frac{1}{8} \right] - \left[ \frac{1}{24} \right] P \cos\theta_P \right). \quad (58)$$

which can be checked to agree with the results in Sec. 5 setting  $y = 0$ .

The helicity no-flip contribution is again obtained by taking the  $m_e \rightarrow 0$  limit in Eqs. (30) - (33) but now for the differences of the respective spectrum functions as specified in Eq. (55). Including the  $O(y^0)$  Born term contributions one obtains

$$\begin{aligned}
\frac{d\Gamma^{nf}}{dx d\cos\theta_P} = & \Gamma_0 \left( x^2(3-2x) + \frac{\alpha}{12\pi} \left\{ - \left[ (1-x)^2(5-2x) \right] - 4x(11-10x+5x^2) \right. \right. \\
& - 6(6-x)x \ln(1-x) - 2(5+12x-15x^2+4x^3) \ln\left(\frac{y}{x}\right) \\
& + 6(3-4x)x^2 \ln\left(\frac{y}{1-x}\right) + 12(3-2x)x^2\sigma \left. \right\} \\
& + \left( x^2(1-2x) + \frac{\alpha}{12\pi} \left\{ \left[ (1-x)^2(1+2x) \right] - 2(3-10x-13x^2+8x^3) \right. \right. \\
& - \frac{2}{x}(4-12x+18x^2-13x^3) \ln(1-x) + 2(1+21x^2-4x^3) \ln\left(\frac{y}{x}\right) \\
& \left. \left. + 6(1-4x)x^2 \ln\left(\frac{y}{1-x}\right) + 12(1-2x)x^2\sigma \right\} \right) P \cos\theta_P, \tag{59}
\end{aligned}$$

where

$$\sigma = -\frac{\pi^2}{3} + 2\text{Li}_2(x) + \ln(x) \ln(1-x) + 2 \ln\left(\frac{x}{1-x}\right) \ln\left(\frac{y}{x}\right). \tag{60}$$

The no-flip contribution agrees with the result presented in Ref. [6]. We have highlighted the anomalous contributions in Eq. (59) by enclosing them in square brackets. When calculating the total spectrum, i.e. when summing the flip and no-flip contributions (56) and (59), the anomalous contributions cancel.

The  $O(\alpha)$  no-flip contribution is much larger than the flip contribution. This is illustrated in Fig. 5 for the electron spectrum in the  $\mu \rightarrow e$  decay where the flip contribution has been multiplied by a factor of 20 in order to make it visible at all. The vanishing of the flip contribution for  $\cos\theta = +1$  at the hard end of the spectrum can be understood from angular momentum conservation. In order to be able to discuss the residual mass dependence the no-flip contribution has been split into its constant part and its logarithmic ( $\ln y$ ) part which come in with opposite signs over most of the spectrum, i.e. they partially cancel in the spectrum. Considering the numerical values of the ratios  $\ln y_{(\tau \rightarrow \mu)} / \ln y_{(\mu \rightarrow e)} = 0.53$  and  $\ln y_{(\tau \rightarrow e)} / \ln y_{(\mu \rightarrow e)} = 1.53$  it is clear from Fig. 5 that the cancellation between the constant and the logarithmic part is strongest for  $\tau \rightarrow \mu$  and

weakest for  $\tau \rightarrow e$ . This observation provides a qualitative explanation of the hierarchy of the size of radiative corrections to the three decay cases as described in Sec. 5, namely the radiative corrections are largest for  $\tau \rightarrow e$  and smallest for  $\tau \rightarrow \mu$ .

We now turn to the discussion of the longitudinal polarization of the daughter lepton in the  $m_e \rightarrow 0$  limit. It takes a rather simple form when one expands out the inverse denominator in terms of powers of  $(\alpha/\pi)$  keeping only the  $O(\alpha)$  contribution. In terms of the flip and no-flip contributions the longitudinal polarization of the electron reads

$$P_e^l = \frac{d\Gamma^{hf} - d\Gamma^{nf}}{d\Gamma^{hf} + d\Gamma^{nf}} \quad (61)$$

When expanding the inverse denominator in terms of powers of  $(\alpha/\pi)$  one sees that the “normal” contributions in the numerator and denominator cancel exactly at  $O(\alpha)$  and one just remains with the anomalous contributions (No such cancellations occur for the forward-backward asymmetry  $A_{FB}$ . We therefore refrain from presenting a closed formula for  $A_{FB}$  in this approximation). One obtains

$$P_e^l = -\left(1 - \frac{\alpha}{6\pi} \frac{(1-x)^2}{x^2} \frac{5-2x - (1+2x)P \cos \theta_P}{3-2x + (1-2x)P \cos \theta_P}\right) \quad (62)$$

It is clear that Eq. (62) does not apply very close to threshold. Due to the factor  $(1-x)^2/x^2$  in (62) the radiative corrections to the longitudinal polarization of the daughter lepton are largest close to threshold as is evidenced in the plots Fig. 2b and Fig. 4b. In the case of  $(\tau \rightarrow \mu)$ , mass effects prevent the radiative corrections to become large in the threshold region.

Integrating the no-flip contribution over the spectrum one obtains

$$\frac{d\langle \Gamma^{nf} \rangle}{d\cos \theta_P} = \Gamma_0 \left( \frac{1}{2} + \frac{\alpha}{\pi} \left( -\left[ \frac{1}{8} \right] + \frac{25}{16} - \frac{1}{4}\pi^2 \right) + \left( -\frac{1}{6} + \frac{\alpha}{\pi} \left( \left[ \frac{1}{24} \right] - \frac{617 - 84\pi^2}{432} \right) \right) P \cos \theta_P \right). \quad (63)$$

which agrees with the results in Sec. 5. In particular one reproduces the simple expression Eq.(51) for the average of the longitudinal polarization. We have again highlighted the anomalous contributions by enclosing them in square brackets. The anomalous contributions can be seen to cancel in the spectrum and rate functions when adding up the spectrum no-flip contribution (59) and flip contribution (56), and the respective rate contributions (63) and (58). Numerically the  $O(\alpha)$  no-flip contribution dominates over the  $O(\alpha)$  (anomalous) flip contribution. For the  $O(\alpha)$  contributions to the rate functions, which do not depend on  $y$  in the  $y \rightarrow 0$  approximation, one obtains  $(-0.168, -0.121, -0.107)$  for the rate ratio  $d\Gamma^{hf(\alpha)}/d\Gamma^{nf(\alpha)}$ , for  $\cos \theta_P = 1, 0, -1$ .

## 7 Summary and conclusions

We have computed the  $O(\alpha)$  corrections to the leptonic decays of the  $\mu^-$  and  $\tau^-$  leptons including polarization effects and the full mass dependence of the respective final-state leptons. The radiative corrections to the spectrum functions are sizeable for  $(\mu \rightarrow e)$ -decays, large for  $(\tau \rightarrow e)$ -decays, and smaller for  $(\tau \rightarrow \mu)$ -decays. In large part this pattern is due to the  $(\ln y)$ -dependent contributions to the spectrum. The polarization of the final-state lepton deviates substantially from the naive  $m_{l'} = 0$  values  $P_{l'}^l = -1$  and  $P_{l'}^\perp = 0$  towards the soft end of the spectrum. The radiative corrections to the longitudinal and transverse polarization of the daughter lepton in the threshold region are substantial for  $(\mu \rightarrow e)$ - and  $(\tau \rightarrow e)$ -decays and small for  $(\tau \rightarrow \mu)$ -decays. Similar statements hold for the forward-backward asymmetry  $A_{FB}$ .

For the rate functions we have compared our  $O(\alpha)$   $m_{l'} \neq 0$  results with  $m_{l'} \rightarrow 0$  results derived previously in [6]. In particular in the  $(\tau \rightarrow \mu)$  case the errors incurred in using the  $O(\alpha)$   $m_{l'} \rightarrow 0$  results are large (of  $O(10\%)$  in the  $O(\alpha)$  rate functions).

Whether one is willing to tolerate the error brought about by using the simpler  $m_{l'} \rightarrow 0$  radiative correction formulas depends of course on the accuracy required for the application at hand. We nevertheless strongly recommend use of the complete results in numerical investigations instead of using the  $m_{l'} \rightarrow 0$  approximation. The analytical  $m_{l'} \neq 0$  formulas written down in this paper are of sufficient simplicity to allow for easy incorporation into numerical programs.

From what was being said in Sec.3 it is clear that the results of this paper can immediately be applied to the case of semileptonic quark decays, where e.g. in the case of the semileptonic  $b \rightarrow c + l^- + \bar{\nu}_l$  decays the final state  $c$ -quark mass can certainly not be neglected.

**Acknowledgements:** We acknowledge informative discussions with F. Scheck, K. Schilcher and H. Spiesberger. We would like to thank A.B. Arbuzov for clarifying e-mail exchanges. M.C. Mauser and S. Groote are supported by the DFG (Germany) through the Graduiertenkolleg ‘‘Eichtheorien’’ at the University of Mainz.

## A Appendix A

When integrating the spectrum functions it is convenient to transform to the integration variable  $\xi$ , where  $x = y(\xi^2 + 1)/\xi$ , such that  $\beta = (1 - \xi^2)/(1 + \xi^2)$ .

Trilog functions are generated from the integrals

$$\int_1^y \frac{1}{\xi} \ln(\xi) \ln(\xi - y) d\xi = \frac{\pi^2}{6} \ln y + \frac{1}{3} \ln^3 y - \text{Li}_3(y) + \zeta(3), \quad (\text{A1})$$

$$\int_1^y \frac{1}{\xi} \ln(\xi) \ln(1 - y\xi) d\xi = -\ln(y) \text{Li}_2(y^2) - \text{Li}_3(y) + \text{Li}_3(y^2), \quad (\text{A2})$$

$$\int_1^y \frac{1}{\xi} \text{Li}_2\left(\frac{y(1 - \xi^2)}{\xi(1 - y\xi)}\right) d\xi = \frac{1}{2} \ln(y) \text{Li}_2(y^2) + 2 \text{Li}_3(y) - \text{Li}_3(y^2) - \zeta(3), \quad (\text{A3})$$

$$\int_1^y \frac{1}{\xi} \text{Li}_2\left(\frac{1 - \xi^2}{1 - y\xi}\right) d\xi = \frac{\pi^2}{6} \ln y - \frac{1}{2} \ln(y) \text{Li}_2(y^2) - 2 \text{Li}_3(y) + \text{Li}_3(y^2) + \zeta(3), \quad (\text{A4})$$

where

$$\text{Li}_2(x) := -\int_0^1 \frac{\ln(1 - y)}{y} dy, \quad \text{Li}_3(x) := \int_0^1 \frac{\text{Li}_2(y)}{y} dy. \quad (\text{A5})$$

Use has been made of the relation

$$\text{Li}_n(x) + \text{Li}_n(-x) = \frac{1}{2^{n-1}} \text{Li}_n(x^2). \quad (\text{A6})$$

Euler's *Zeta* function is defined by

$$\zeta(s) = \sum_{k=1}^{\infty} k^{-s}, \quad \zeta(3) = 1.202057\dots \quad (\text{A7})$$

## B Appendix B

The Fierz identity

$$[\gamma^\mu(1 - \gamma_5)]_{\alpha\beta} [\gamma_\mu(1 - \gamma_5)]_{\gamma\delta} = -[\gamma^\mu(1 - \gamma_5)]_{\gamma\beta} [\gamma_\mu(1 - \gamma_5)]_{\alpha\delta} \quad (\text{B1})$$

is well known. Not so well known is the Fierz identity (see e.g. [10])

$$[(1 \pm \gamma_5)]_{\alpha\beta} [(1 \mp \gamma_5)]_{\gamma\delta} = \frac{1}{2} [\gamma^\mu(1 \mp \gamma_5)]_{\gamma\beta} [\gamma_\mu(1 \pm \gamma_5)]_{\alpha\delta}. \quad (\text{B2})$$

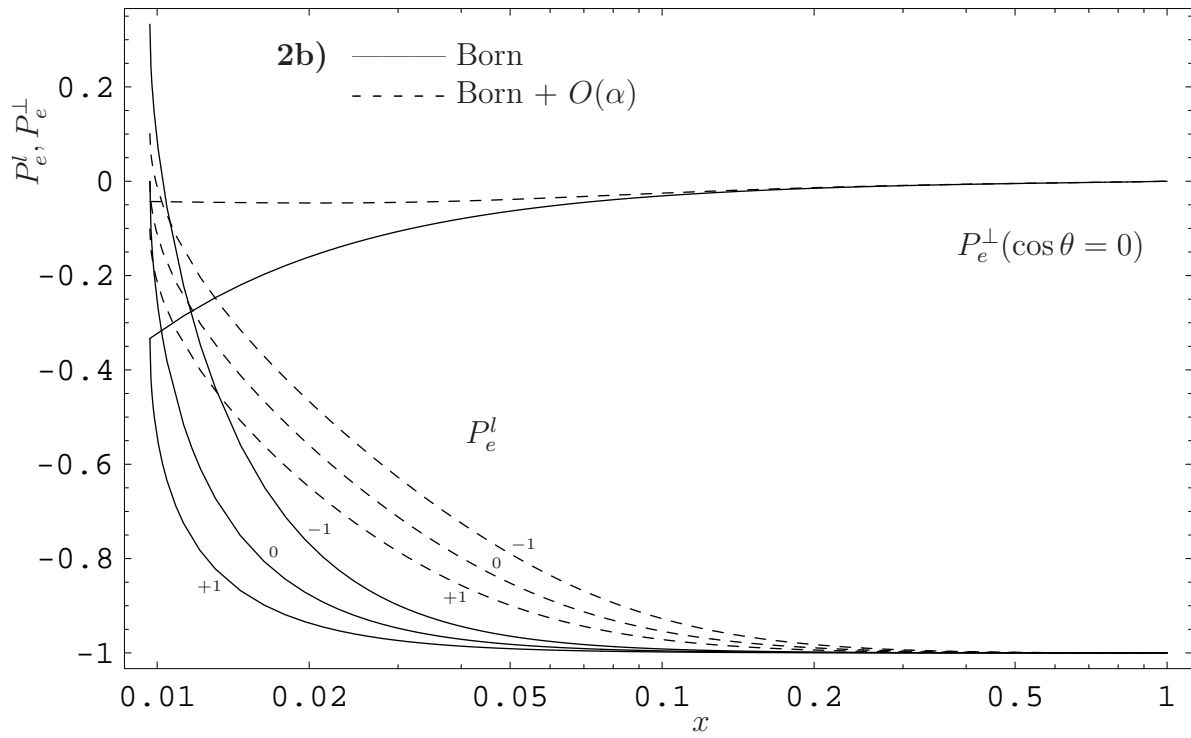
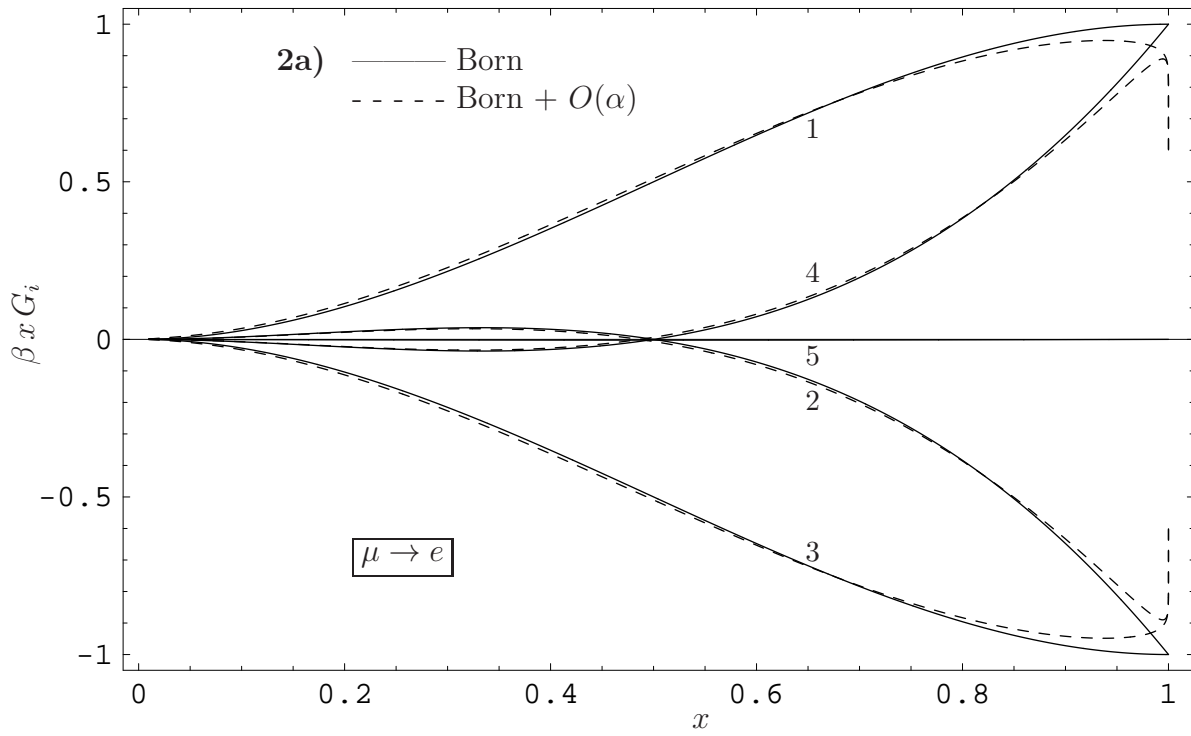
Latter identity allows one to transform the  $q^\mu q^\nu$  piece of the  $W$ -boson propagator discussed in Sec. 4 back into the standard form  $N^{\alpha\beta} C_{\alpha\beta}$  used in the remaining part of the paper.

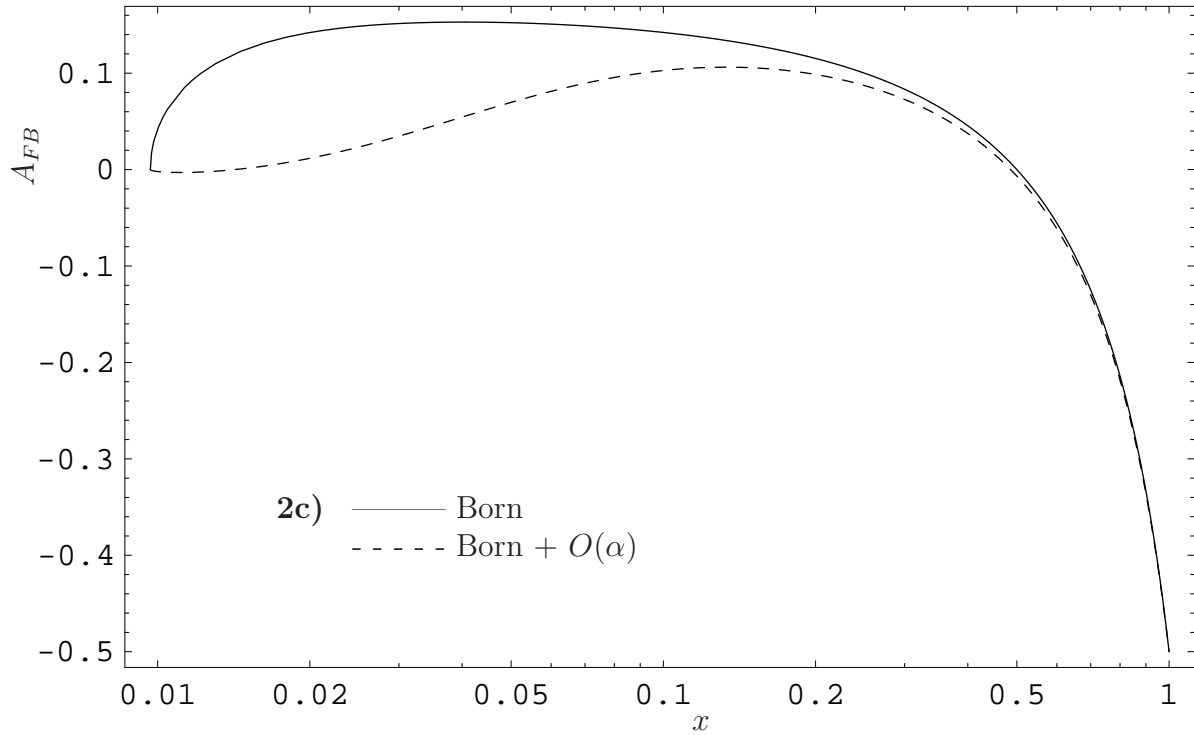
## References

- [1] M. Fischer, S. Groote, J.G. Körner and M.C. Mauser, Phys. Lett. **B480** (2000) 265.
- [2] M. Fischer, S. Groote, J.G. Körner and M.C. Mauser, Phys. Rev. **D65** (2002) 013205.
- [3] T.D. Lee and M. Nauenberg, Phys. Rev. **133B** (1964) 1549.
- [4] R. Kleiss, Z. Phys. C **33** (1987) 433;  
A.V. Smilga, Commun. Nucl. Part. Phys. **20** (1991) 69;  
J.G. Körner, A. Pilaftsis and M.M. Tung, Z. Phys. **C63** (1994) 575;  
S. Groote, J.G. Körner and M.M. Tung, Z. Phys. **C74** (1997) 615;  
S. Groote, J.G. Körner and J.A. Leyva, Phys. Lett. **B418** (1998) 192;  
L. Trentadue and M. Verbeni, Phys. Lett. **B478** (2000) 137 and  
Nucl. Phys. **B583** (2000) 307;  
S. Dittmaier and A. Kaiser, Phys. Rev. **D65**, 113003 (2002).
- [5] B. Falk and L.M. Sehgal, Phys. Lett. **B325** (1994) 509.
- [6] W.E. Fischer and F. Scheck, Nucl. Phys. **B83** (1974) 25.
- [7] A.B. Arbuzov, Phys. Lett. **B524** (2002) 99.
- [8] G. Källén, “Elementary Particle Physics”, Addison–Wesley Publishing Company, Reading, Massachusetts, USA, 1964.
- [9] E.D. Commins and P.H. Bucksbaum, “Weak Interactions of Leptons and Quarks”, Cambridge University Press, Cambridge, U.K., 1983.
- [10] F. Scheck, “Leptons, Hadrons and Nuclei”, North Holland Physics Publishing, Amsterdam, 1983.
- [11] T.D. Lee and C.S. Wu, Annual Review of Nuclear Science **15** (1965) 381;  
*ibid* **16** (1966) 471.
- [12] G. Källén, Springer Tracts in Modern Physics **46** (1968) 67.
- [13] F. Scheck, Phys. Rep. **44** (1978) 187.

- [14] M. T. Mehr and F. Scheck, Nucl.Phys. **B149** (1979) 123.
- [15] M. Roos and A. Sirlin, Nucl. Phys. **B29** (1971) 296.
- [16] D. E. Groom *et al.* [Particle Data Group Collaboration],  
Eur. Phys. J. **C19** (2000) 1.
- [17] W. J. Marciano and A. Sirlin, Phys. Rev. Lett. **61** (1988) 1815.
- [18] K. Schilcher, M.D. Tran and N.F. Nasrallah, Nucl.Phys. **B181** (1981) 91,  
Erratum *ibid.* **B187** (1981) 594;  
G.J. Gounaris and J.E. Paschalis, Nucl. Phys. **B222** (1983) 473.
- [19] T. Kinoshita, “Everyone makes mistakes - including Feynman”,  
J. Phys. **G29** (2003) 9.
- [20] E. Kuraev and V.S. Fadin, Sov. J. Nucl. Phys. **41** (1985) 466,  
[Yad. Fiz. 41 (1985) 733].
- [21] M. Cacciari, A. Deandrea, G. Montagna and O. Nicrosini,  
Europhys. Lett. **17** (1992) 123.
- [22] Y. Nir, Phys. Lett. **B221** (1989) 184.
- [23] T. van Ritbergen and R.G. Stuart, Nucl. Phys. **B564** (2000) 343.
- [24] A.D. Dolgov and V.I. Zakharov, Nucl. Phys. **B27** (1971) 525.







**Figures 2a, b, c:**

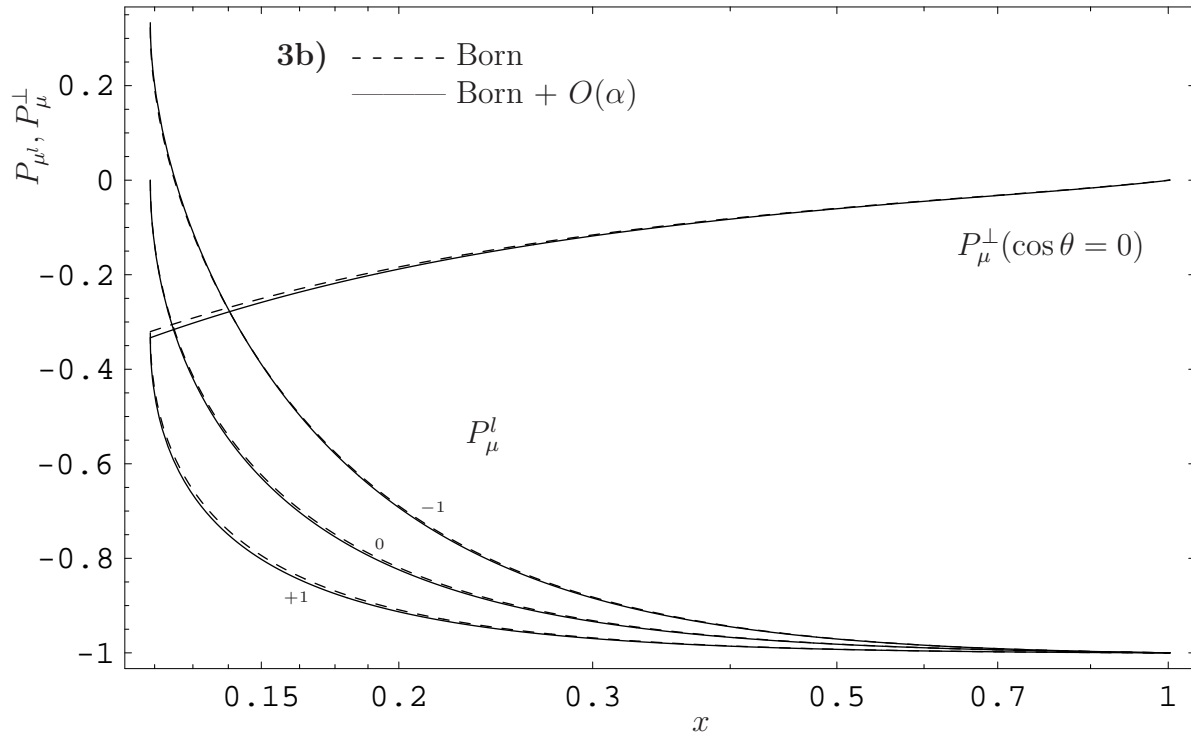
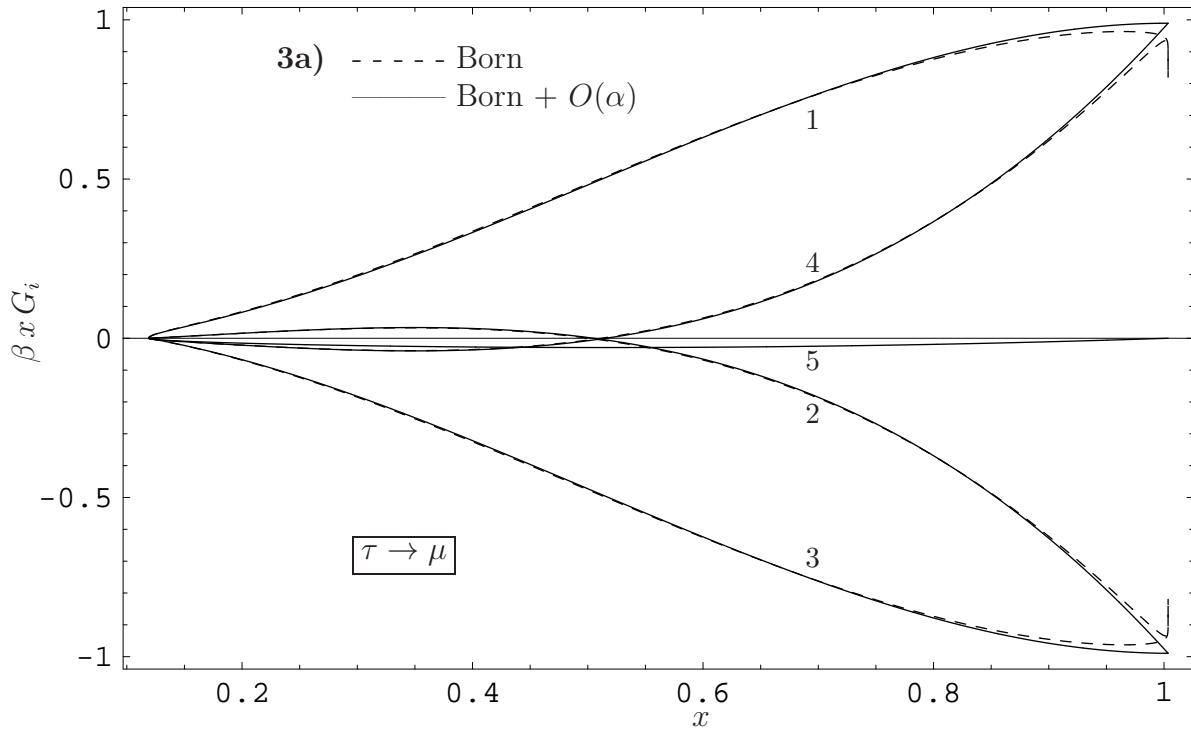
The case  $\mu \rightarrow e$ . Scaled energy dependence of

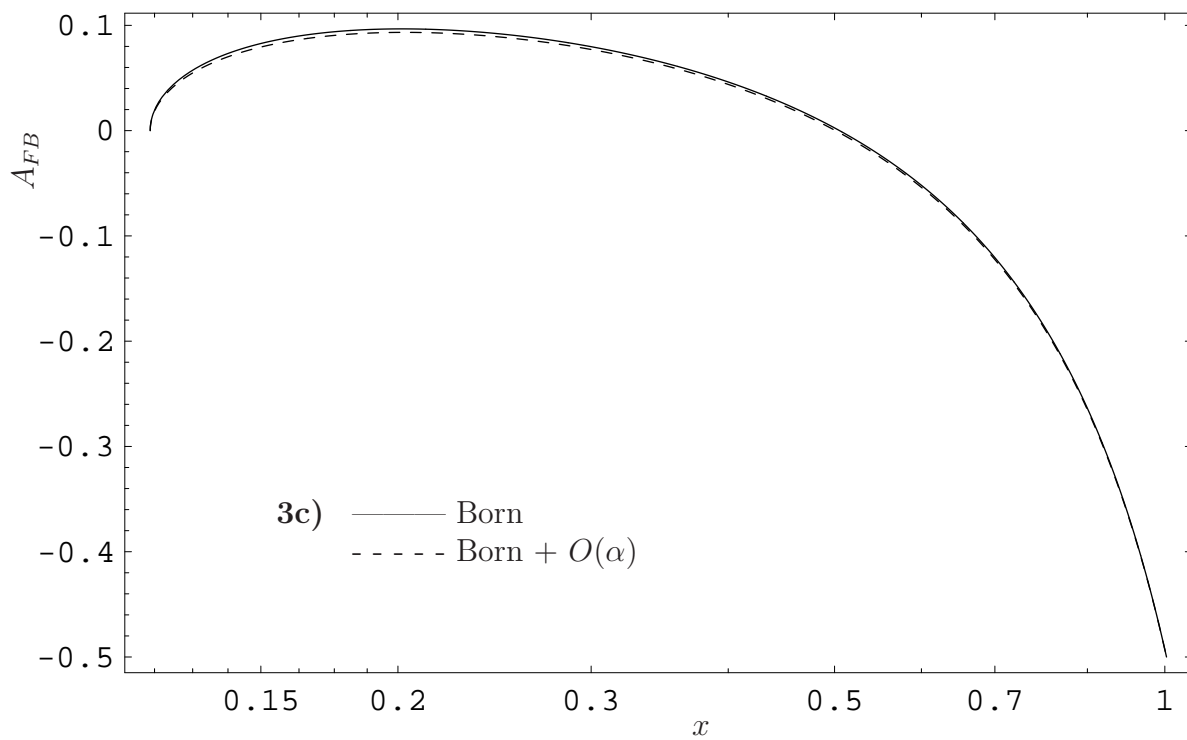
a) spectrum functions  $\beta x G_i$ ,  $i = 1, \dots, 5$

b) the longitudinal polarization of the electron  $P_e^l$  for  $\cos \theta_P = -1, 0, +1$ , and

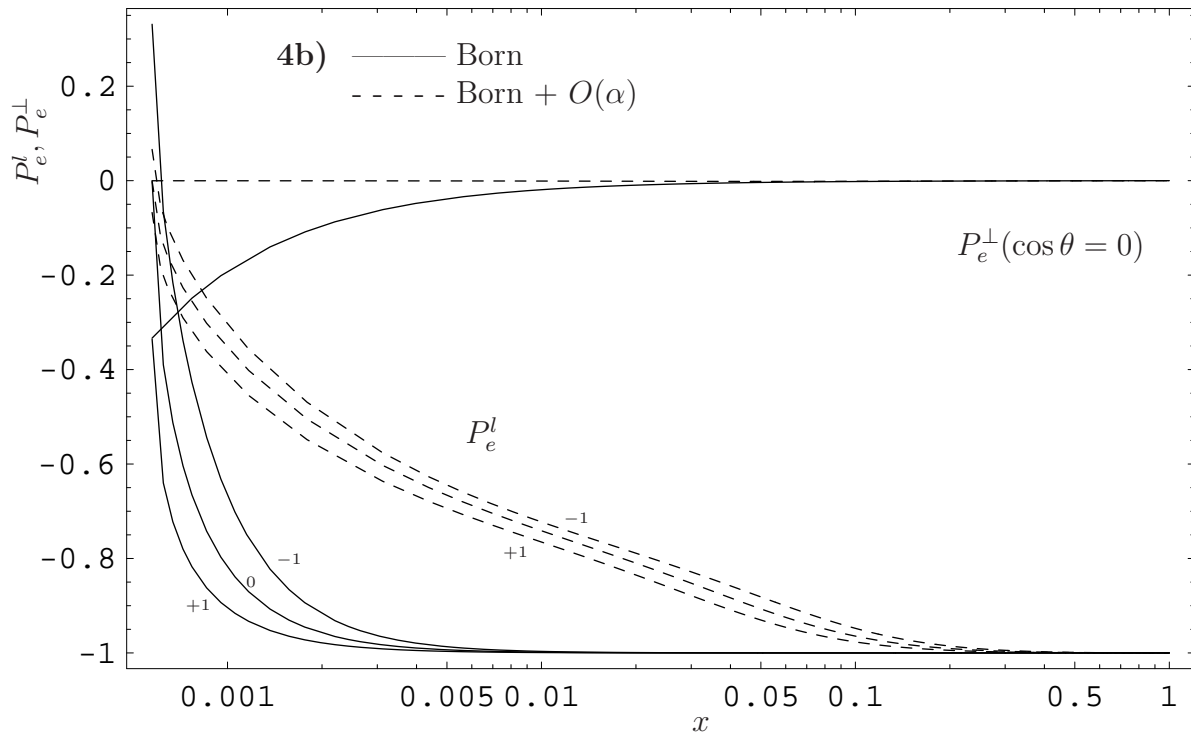
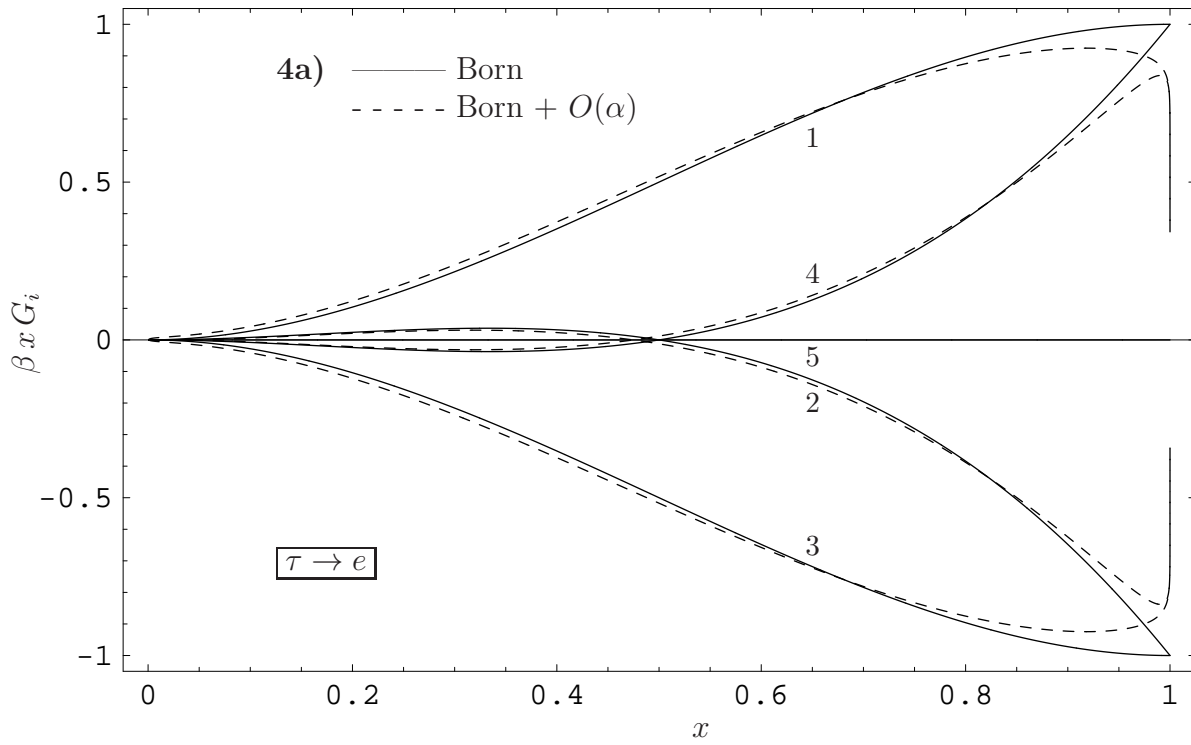
c) the forward-backward asymmetry  $A_{FB}$  for  $\cos \theta = 0$ .

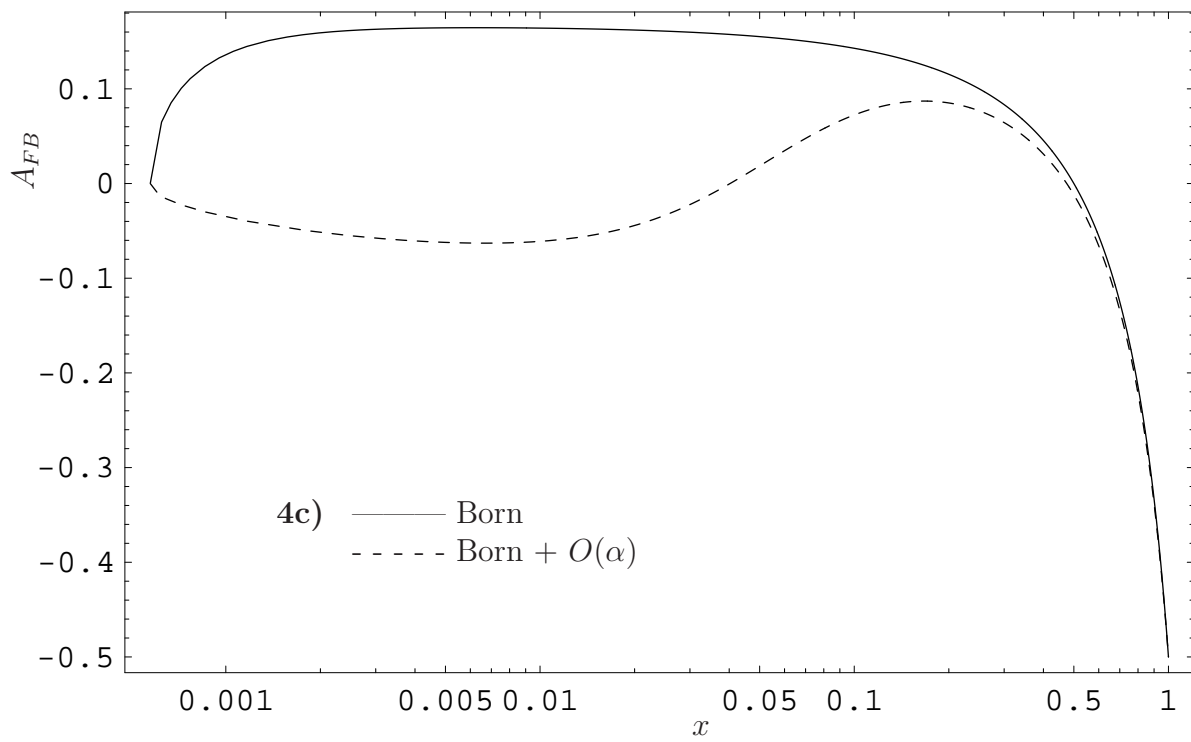
All curves with and without radiative corrections. Polarisation  $P$  is set to  $P = 1$ .





**Figures 3a, b, c:**  
 The case  $\tau \rightarrow \mu$ . Caption as in Fig. 2.





**Figures 4a, b, c:**  
 The case  $\tau \rightarrow e$ . Caption as in Fig. 2.

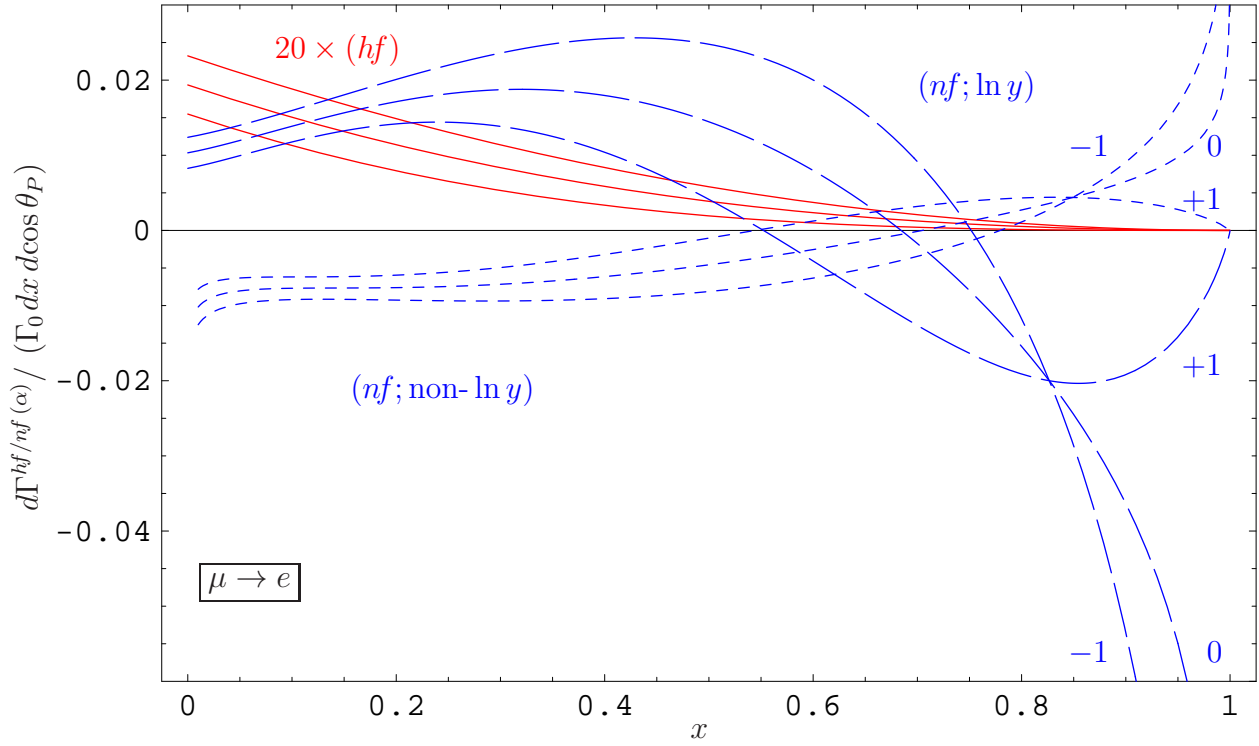


**Figure 5:**

Scaled energy dependence of flip ( $hf$ ) and no-flip ( $nf$ ) spectrum functions in the limit  $y \rightarrow 0$ . Latter contribution is separated into its non-logarithmic part ( $nf; \text{non-} \ln y$ ) and its mass dependent logarithmic part ( $nf; \ln y$ ) which is plotted for the case ( $\mu \rightarrow e$ ).